

Stand structure and recent climate change constrain stand basal area change in European forests: a comparison across boreal, temperate and Mediterranean biomes

Journal:	<i>Ecosystems</i>
Manuscript ID:	ECO-13-0326.R3
Types:	Original Article
Date Submitted by the Author:	n/a
Complete List of Authors:	<p>Ruiz-Benito, Paloma; University of Stirling, Biological and Environmental Sciences; University of Alcala, Forest Ecology and Restoration Group, Department of Life Sciences; Forest Research Center - Instituto Nacional de Investigación y Tecnología Agraria y Alimentaria (CIFOR-INIA, Department of Forest Ecology and Genetics</p> <p>Madrigal-Gonzalez, Jaime; University of Alcala, Forest Ecology and Restoration Group, Department of Life Sciences</p> <p>Ratcliffe, Sophie; University of Leipzig, AG Spezielle Botanik und Funktionelle Biodiversität</p> <p>Coomes, David; University of Cambridge, Plant Sciences</p> <p>Kaendler, Gerald; The Forest Research Institute,</p> <p>Lehtonen, Aleks; Metla, Carbon</p> <p>Wirth, Christian; University of Leipzig, AG Spezielle Botanik und Funktionelle Biodiversität; German Centre for Integrative Biodiversity Research (iDiv),</p> <p>Zavala, Miguel; University of Alcala, Forest Ecology and Restoration Group, Department of Life Sciences</p>
Key Words:	carbon sink, climatic variability, competition, inventory-based data, minimum temperature, mixed models, stand basal area change, water availability

1 Stand structure and recent climate change constrain stand basal area change in
2 European forests: a comparison across boreal, temperate and Mediterranean
3 biomes

4 Short title: Drivers of basal area change across Europe

5 P. Ruiz-Benito^{1,2,3*}, J. Madrigal-González² (ecojmg@hotmail.com), S. Ratcliffe⁴
6 (sophia.ratcliffe@uni-leipzig.de), D. A. Coomes⁵ (dac18@cam.ac.uk), G. Kändler⁶
7 (Gerald.Kaendler@forst.bwl.de), A. Lehtonen⁷ (aleksi.lehtonen@metla.fi), C. Wirth^{4,8}
8 (cwirth@uni-leipzig.de), M. A. Zavala² (madezavala@gmail.com),

¹*Department of Forest Ecology and Genetics, ForestResearch Center - Instituto Nacional de Investigación y Tecnología Agraria y Alimentaria (CIFOR-INIA), Ctra. de la Coruña, Km. 7,5. 28040. Madrid, Spain.*

²*Forest Ecology and Restoration Group, Department of Life Sciences, Science Building, University of Alcalá, Campus Universitario, 28871, Alcalá de Henares (Madrid), Spain.*

³*Biological and Environmental Sciences, School of Natural Sciences, University of Stirling. FK9 4LA, Stirling, United Kingdom.*

⁴*University of Leipzig. AG Spezielle Botanik und Funktionelle Biodiversität. Johannisallee 21-2. 04103 Leipzig, Germany.*

⁵*Forest Ecology and Conservation Group, Department of Plant Sciences, University of Cambridge, Downing Street, Cambridge, CB3 2EA, UK.*

⁶*The Forest Research Institute, Wonnhaldestr. 4. 79100 Freiburg, Germany.*

⁷*Finnish Forest Research Institute, Vantaa Research Centre, PO Box 18, 01301 Vantaa, Finland.*

⁸*German Centre for Integrative Biodiversity Research (iDiv) Halle-Jena-Leipzig, Deutscher Platz 5e, 04103 Leipzig, Germany.*

Correspondence: Paloma Ruiz Benito. E-mail: palomaruibenito@gmail.es. Phone: 00 34 637 19 43 53. Fax: 00 34 91 357 22 93.

Type of paper: Original Article

Authorship: JM, PRB and MAZ conceived the design; DC, GK, AL, SR, PRB, CW and MAZ collected the data; JM, PRB and SR analyzed data; DC, JM, SR and PRB contributed to the methods, and all the authors wrote the article.

For Peer Review

1
2
3
4
5
6
7
8
9
10
11
12
13
14
15
16
17
18
19
20
21
22
23
24
25
26
27
28
29
30
31
32
33
34
35
36
37
38
39
40
41
42
43
44
45
46
47
48
49
50
51
52
53
54
55
56
57
58
59
60

ABSTRACT

European forests have a prominent role in the global carbon cycle and an increase in carbon storage has been consistently reported during the 20th century. Any further increase in forest carbon storage, however, could be hampered by increases in aridity and extreme climatic events. Here we use forest inventory data to identify the relative importance of stand structure (stand basal area and mean d.b.h.), mean climate (water availability) and recent climate change (temperature and precipitation anomalies) on forest basal area change during the late 20th century in three major European biomes. Using linear mixed-effects models we observed that stand structure, mean climate and recent climatic change strongly interact to modulate basal area change. Although we observed a net increment in stand basal area during the late 20th century, we found the highest basal area increments in forests with medium stand basal areas and small to medium sized trees. Stand basal area increases correlated positively with water availability, and were enhanced in warmer areas. Recent climatic warming caused an increase in stand basal area, but this increase was offset by water availability. Based on recent trends in basal area change we conclude that the potential rate of aboveground carbon accumulation in European forests strongly depends on both stand structure and concomitant climate warming, adding weight to suggestions that European carbon stocks may saturate in the near future.

Keywords: carbon sink, climatic variability, competition, inventory-based data, minimum temperature, mixed models, water availability, stand basal area change.

53 INTRODUCTION

54 Forests cover more than 30% of the global land surfaces (FRA, 2010), store large
55 reservoirs of carbon (Goodale and others 2002; Pan and others 2011), harbour around
56 two thirds of terrestrial biodiversity (Millennium Ecosystem Assessment 2005) and
57 promote multiple ecosystem services (Gamfeldt and others 2013). Forests play a central
58 role in the global carbon cycle, but the factors controlling terrestrial carbon exchanges
59 and their magnitude remain controversial (Valentini and others 2000; Nabuurs and
60 others 2003; Bellassen and Luyssaert 2014). For example, it is widely accepted that
61 current increases in forest biomass observed in many temperate forests result partially
62 from positive effects of global change (e.g. Pastor and Post 1988; Nabuurs and others
63 2003; Ciais and others 2008; Hember and others 2012; Peng and others 2014) and
64 changes in forest management regimes (e.g. Spiecker 1999; Luyssaert and others 2010),
65 but the influences of climate change and extreme climatic events on biomass changes
66 are not well understood (Dixon and others 1994; Schimel 2007; McMahon and others
67 2010).

68 Future forest carbon sinks could be affected by large-scale changes in mortality
69 and growth rates, both of which are related to climate, forest structure and the
70 interactions between these factors (e.g. van Mantgem and others 2009; Dietze and
71 Moorcroft 2011; Ruiz-Benito and others 2013). The rate of increase in carbon storage
72 depends on forest structure, climate warming, CO₂ fertilisation and nitrogen deposition
73 effects (Nabuurs and others 2003; Ciais and others 2008; Pan and others 2011).
74 Although the magnitude of these effects remains uncertain, it has been shown that
75 recent climate change and CO₂ fertilisation could have a positive impact on tree growth
76 (Cao and Woodward 1998; Ciais and others 2008; Bellassen and others 2011).
77 However, these positive effects could be overwhelmed by the effects of increased

1
2
3
4
5
6
7
8
9
10
11
12
13
14
15
16
17
18
19
20
21
22
23
24
25
26
27
28
29
30
31
32
33
34
35
36
37
38
39
40
41
42
43
44
45
46
47
48
49
50
51
52
53
54
55
56
57
58
59
60

78 climatic variability and extreme climatic events, such as more frequent and more intense
79 drought events (e.g. Ciais and others 2005; Zhao and Running 2010; Hoch and Körner
80 2012). Moreover, regional studies have not shown consistent trends in forest growth
81 rates; growth is increasing in temperate areas but no clear trends have been found in
82 European boreal or Mediterranean forests (Spiecker, 1999). On the other hand, recent
83 worldwide episodes of increased defoliation and tree mortality have been related to
84 climate-induced processes (Allen and others 2010; Carnicer and others 2011). Forest
85 carbon sinks could be potentially affected by large-scale changes in mortality and
86 growth rates, both of which have been related to climate and/or its interaction with
87 forest structure (e.g. van Mantgem and others 2009; Dietze and Moorcroft 2011; Ruiz-
88 Benito and others 2013).

89 European forests have been globally important carbon sinks (Ciais and others
90 2008; Nabuurs and others 2003), but what will happen in future is a matter of intense
91 debate (Narbuurs and others 2013). As a result of climate change, mean temperatures
92 are likely to increase, with northern Europe experiencing warmer winters and
93 Mediterranean regions warmer summers (Christensen and others 2007). Meanwhile,
94 climate change scenarios suggest that precipitation could increase in northern Europe
95 and decrease in Mediterranean regions (Christensen and others 2007). The exposure of
96 Mediterranean systems to even hotter, drier summers could result in the death of trees
97 normally regarded as drought tolerant, because the combination of low soil moisture
98 potentials and strong vapour pressure deficits push water transport systems to their limit
99 (Allen and others 2010; Ruiz-Benito and others 2013). Thus, climate change could
100 result in a reduction of carbon gains in the water-limited forests of Europe (Vayreda and
101 others 2012), that could even counteract gains arising from the abandonment of
102 agricultural lands (Canadell and Raupach 2008).

Understanding how forest structure and climate interact to drive biomass change across European forests, from boreal to temperate and Mediterranean forests is critical to infer future trends in forest carbon sinks. The role of European forests in the global carbon cycle in the second half of the 20th century has been largely estimated through inventory-based national statistics (e.g. Goodale and others 2002; Nabuurs and others 2003; Ciais and others 2008; Bellassen and others 2011). Recently tree level information from consecutive inventories has become available in a growing number of EU countries, allowing us to better estimate large-scale demographic processes (e.g. Kunstler and others 2011; Benito-Garzón and others 2013; García-Valdés and others 2013, Vilà and others 2013). In this study we performed, for the first time, a large-scale analysis of the main patterns and drivers of recent stand basal area change in the three main biomes of European forests, using plot-level forest inventory information. Our specific objectives were: (i) to examine recent decadal patterns of forest basal area change, growth and mortality across Mediterranean, temperate and boreal biomes in Europe; and (ii) to quantify the effect of stand structure, mean climate and recent climate change on stand basal area change.

MATERIAL AND METHODS

Data of stand basal area change and its components

We compiled information from consecutive National Forest Inventories (NFI hereafter) of Spain, Germany and Finland (see methodological details in Appendix 1 of supplementary material), which encompass stands belonging to Mediterranean, temperate and boreal biomes (Figure 1a). We selected plots from consecutive surveys where tree-level data on ingrowth, surviving and dead trees was recorded in both surveys (see supplementary Appendix 1 and Table S1).

1
2
3
4
5
6
7
8
9
10
11
12
13
14
15
16
17
18
19
20
21
22
23
24
25
26
27
28
29
30
31
32
33
34
35
36
37
38
39
40
41
42
43
44
45
46
47
48
49
50
51
52
53
54
55
56
57
58
59
60

127 From the initial plots of the three NFIs we selected a total of 40,521 plots where
128 at least one adult tree was measured (i.e. d.b.h. > 10 cm) and where there was no
129 evidence of thinning or harvesting in either of the two consecutive surveys. Plots with
130 any sign of harvesting were excluded for two reasons: (i) biomass loss due to harvesting
131 implies an assessment of growth considering only surviving trees, which could result in
132 biased estimates of real productivity in natural forests-; and (ii) harvesting usually
133 triggers an immediate growth release in neighbouring trees and, therefore, management
134 could affect carbon stock changes (Vayreda and others 2012).

135 In the 40,521 plots each tree alive in the first inventory was recorded as either
136 alive or dead in the second inventory. We estimated the absolute change in basal area
137 and the relative growth and mortality rates in each plot. Thus, we calculated: (i) stand
138 basal area change ($\text{m}^2 \text{ ha}^{-1} \text{ yr}^{-1}$, SBAC hereafter) as the difference in stand basal area
139 between the two surveys with respect to the time interval; (ii) basal area growth rate
140 (annual percentage, SBA_{gain}) as the sum of basal area increments of all live trees present
141 in each survey with respect to the time interval and initial stand basal area; and (iii)
142 basal area loss rate due to natural mortality (annual percentage, SBA_{loss}) as the basal
143 area lost between consecutive surveys due to mortality, again with respect to the initial
144 stand basal area and time interval following Sheil and others (1995). Basal area loss rate
145 was greater than zero in 25.4% of the plots included in this analysis (i.e. from the
146 40,521 measured plots included in this analysis 10,303 had a basal area loss rate greater
147 than zero). We used stand basal area change instead of biomass change directly because:
148 (i) basal area has been identified as reliable a proxy for biomass (e.g. Slik and others
149 2010); (ii) allometric equations do not exist for all 158 species present in the 40,521
150 plots included in the analysis; and (iii) allometric relationships can vary along the large
151 climatic gradient covered in this study (e.g. Lines and others 2012). We produced maps

of SBA_c , SBA_{gain} and SBA_{loss} using ArcGIS 10 (ESRI Inc., Redlands, CA, USA; Figure 1).

Forest structure and climate data

We used two forest structure variables, two climatic variables and two variables representative of recent climatic change as potential predictors of recent stand basal area changes. Mean tree diameter (d_m , mm) and stand basal area (BA , $m^2 ha^{-1}$), in the first survey, were used to represent forest structure.

To characterise the spatial variability of climate across the three biomes, for each of the plots we obtained climatic variables from WorldClim (Hijmans and others 2005) and CGIAR-CSI GeoPortal, using CGIAR-CSI Global-Aridity and Global-PET Database (Zomer and others 2007; 2008). Two climatic variables were selected to characterise the climate in each plot (see details of variable selection in supplementary Appendix 2 and Table S2): an index of water availability (WAI) and mean temperature of the coldest quarter (hereafter minimum temperature, T_{min}) (based on data between 1950 and 2000). WAI integrates temperature and rainfall in each plot (i.e. annual precipitation minus potential evapotranspiration divided by potential evapotranspiration). Negative values of WAI correspond to dry areas and positive values to wet areas, and it has been shown to be an important driver of tree carbon storage in the Mediterranean region (Vayreda and others 2012). Minimum temperature is thought to be an important constraint in eastern European limits of tree species distribution (e.g. Sykes and Prentice 1996).

The magnitude of recent climate change was quantified by comparing mean annual temperature and precipitation over the study period with the mean of each climatic variable over the reference period 1900-2006, using mean monthly climate data

1
2
3
4
5
6
7
8
9
10
11
12
13
14
15
16
17
18
19
20
21
22
23
24
25
26
27
28
29
30
31
32
33
34
35
36
37
38
39
40
41
42
43
44
45
46
47
48
49
50
51
52
53
54
55
56
57
58
59
60

at 0.5 x 0.5 degree resolution from UDel_AirT_Precip data provided by the NOAA/OAR/ESRL PSD (Boulder, Colorado, USA). The study period was defined as the number of years between the two consecutive inventories plus two years before the first survey (i.e. 1984-2006 Spain; 1984-2002 Germany; 1983-1995 Finland) to include lagged effects of climate on growth or mortality (Vayreda and others 2012). We calculated absolute temperature anomalies and relative precipitation anomalies, using yearly averages calculated using mean monthly climate data (i.e. from January to December). The absolute temperature anomaly (°C) was defined as the difference between the mean temperature for the study period and the mean value for the reference period (1900-2006). The relative precipitation anomaly (%) was defined as the ratio between the equivalent differences for precipitation and the mean value for precipitation for the reference period. The absolute temperature anomalies varied from -0.3 to 1 °C among grid cells (with an average increment of 0.46 °C), while the relative precipitation anomalies varied from -18.7% to 14.6% (with an average of -2.5%, see supplementary Figure S1 and S2).

Statistical analyses

We modelled stand basal area change (SBAc, m² ha⁻¹ yr⁻¹) using linear mixed-effects models, with a Gaussian distribution of residuals and used an identity link for the response variable. All analyses were performed in R version 2.15.1 (R Core Team 2012), using the “lme4” package (Bates and others 2012).

The six fixed predictor variables of SBAC used were: stand basal area (BA, m²/ha), mean d.b.h. (d_m, mm), water availability (WAI, %), minimum temperature (T_{min}, °C), absolute temperature anomaly (TA, °C) and relative precipitation anomaly (PA, %) (see mean values in supplementary Figure S3 and Table S3). Due to the

clustered nature of the sampling in Finland and Germany (where plots are aggregated in groups of four; see Appendix 1 for more information), we included cluster as a random effect in the model. We fitted country as a fixed effect because it only has three levels, and as such is inappropriate as a random effect (see Bolker and others 2009). Our full model also included as fixed effects linear and quadratic terms for each explanatory variable. Based on our initial hypothesis we also included pair-wise interactions between stand structure and climate variables: $d_m \times BA$, $WAI \times T_{min}$, $BA \times WAI$, $BA \times T_{min}$, $BA \times TT$, $BA \times PT$, $d_m \times WAI$, $d_m \times T_{min}$, $d_m \times TT$, $d_m \times PT$ and $WAI \times TT$, $WAI \times PT$ and $T_{min} \times TT$. All the numerical predictor variables were standardised (i.e. the mean was subtracted from each value and divided by the standard deviation), enabling the interactions to be included in the model (Zuur and others 2009). Additionally, in order to detect collinearity between explanatory variables, we calculated the variance inflation factors (VIFs) for each predictor variable. VIFs calculate the degree to which collinearity inflates the estimated regression coefficients as compared with the orthogonal predictors (Belsey, 1991; Oksanen and others 2010). Our results confirmed that collinearity was not a major problem in our data ($VIF < 3$).

The most parsimonious model was determined using BIC (Bayesian Information Criterion) as an indicator of both parsimony and likelihood (Burnham and Anderson 2002). To identify the best-supported model we first constructed candidate models in which each of the interactions were dropped and if the difference in BIC between the reduced and full models was less than two then the simpler model was selected (Hilborn and Mangel 1997; Pinheiro and Bates 2000). The process was then repeated for all the independent variables this time comparing each individual predictor variable with a model containing all response variables without any interactions, using the differences in BIC to quantify the relative importance of each predictor variable. Finally, parameter

1
2
3
4
5
6
7
8
9
10
11
12
13
14
15
16
17
18
19
20
21
22
23
24
25
26
27
28
29
30
31
32
33
34
35
36
37
38
39
40
41
42
43
44
45
46
47
48
49
50
51
52
53
54
55
56
57
58
59
60

225 estimates and confidence intervals of the best-supported model were obtained using
226 restricted maximum likelihood (REML), which minimizes the likelihood of the
227 residuals from the fixed-effect portions of the model (Zuur and others 2009).

228 The marginal R^2 (proportion of variance explained by fixed factors) and
229 conditional R^2 (proportion of variance explained by both the fixed and random factors)
230 were estimated following Nakagawa and Schielzeth (2013). The parameter estimates
231 provide the basis for determining the magnitude of the effect of a given process, with
232 maximum likelihood estimates of parameter values close to zero indicating no effect.
233 Mean parameter estimates and 95% confidence intervals for the fixed effects were
234 estimated using bootstrapping methods available in the lme4 package (Bates and others
235 2012).

236 Response curves for each explanatory variable (varying between the 99%
237 percentiles observed in the data) were computed using the best supported model, fixing
238 the values of the other continuous variables at the observed mean (Table 1), and the
239 categorical variables to zero (i.e. the fixed country effect, Eq. (1)). Approximate
240 confidence intervals of the prediction were calculated from the variance-covariance
241 matrix of the fixed effects ($\pm 2 \times$ standard error of prediction). Response curves were
242 also computed with two variables varying between the 99% percentiles observed in the
243 data, with the rest held constant to the mean; these were visualised using three-
244 dimensional graphs.

RESULTS

Patterns of stand basal area change and its components

During the late 20th century there were positive mean stand basal area changes (SBAc) in the Mediterranean, temperate and boreal biomes (Table 1, supplementary Table S3), confirming that forests in these regions were accumulating basal area at a mean relative annual rate of 3.82%. We observed the largest mean SBAc, growth and loss rates in the temperate biome (Table 1, Figure 1b-d), with the highest basal area loss rates occurring in Spanish temperate forests (i.e. Northern Iberian Peninsula, see Figure 1d and supplementary Table S3). Forests with negative or near-zero SBAc were mainly concentrated in the Mediterranean and northern boreal regions (Table 1, Figure 1b). There was a positive correlation between SBAc and relative basal area gains due to growth ($r = 0.41$, $P < 0.001$, Figure 1b,c), but SBAc was also affected by natural mortality as it can be observed by the negative correlation between SBAc and basal area loss ($r = -0.26$, $P < 0.001$, Figure 1b,d).

A latitudinal gradient in water availability (WAI) and minimum temperature was observed (supplementary Figure S1). The Mediterranean biome had the driest areas (i.e. negative WAI) with increasing water availability towards the temperate and boreal biomes (Table 1), and minimum temperatures were lowest in the boreal biomes (Table 1). Regarding climatic anomalies in the late 20th century, the largest temperature increments and precipitation reductions tended to be concentrated in Mediterranean and cool temperate biomes (Table 1 and supplementary Figure S1).

Effects of stand structure, climate and recent climate change on basal area change

1
2
3 268 The best-supported model included the effects of all predictor variables (marginal $R^2 =$
4
5 269 0.2743 , conditional $R^2 = 0.3761$) and took the following functional form:
6
7
8 270
9
10 271 $SBAc = \beta_1 + \beta_2(BA) + \beta_3(BA^2) + \beta_4(d_m) + (\beta_5(d_m^2) + \beta_6(WAI) + \beta_7(Tmin) +$
11
12 272 $\beta_8(Tmin^2) + \beta_9(TA) + \beta_{10}(PA) + (\beta_{11}PA^2) + \beta_{12}(SP) + \beta_{13}(FI) + \beta_{14}(BA)(d_m) +$
13
14 273 $\beta_{15}(WAI)(Tmin) + \beta_{16}(BA)(WAI) + \beta_{17}(BA)(Tmin) + \beta_{18}(BA)(TA) + \beta_{19}(BA)(PA) +$
15
16 274 $\beta_{20}(d_m)(WAI) + \beta_{21}(d_m)(Tmin) + \beta_{22}(d_m)(TA) + \beta_{23}(d_m)(PA) + \beta_{24}(WAI)(TA) +$
17
18 275 $\beta_{25}(WAI)(PA) + (\beta_{26}(Tmin)(TA)$ (1)
19
20
21
22
23 276
24
25 277 where the response variable is the absolute stand basal area change (SBAc), and the
26
27 278 numerical predictor variables were: stand basal area (BA), mean d.b.h. (d_m), minimum
28
29 279 temperatures (Tmin) and precipitation anomalies (PA) as quadratic terms; and water
30
31 280 availability (WAI) and temperature anomalies (TA) as linear terms (see Table 2 and
32
33 281 supplementary Table S4 for model comparisons, Table 3 for fitted parameter values,
34
35 282 supplementary Figure S4 for observed and predicted SBAC and supplementary Figure
36
37 283 S5 for model residuals). Country (i.e. Spain, Germany and Finland) was included as a
38
39 284 fixed categorical effect and thus linear terms were also included for Spain (SP) and
40
41 285 Finland (FI).
42
43
44
45
46 286 BIC model comparisons indicated that mean d.b.h. had the largest effect on
47
48 287 SBAC, followed by WAI, stand basal area, temperature anomaly and minimum
49
50 288 temperature (Table 2). The relative precipitation anomaly explained the smallest
51
52 289 variation compared to the rest of explanatory variables (Table 2). With regards to the
53
54 290 interaction terms, it is important to note that the full model included all possible pair-
55
56 291 wise interactions between the stand structure and climatic variables, but also strong
57
58 292 interactions between climate and recent climatic anomalies were found (Table 2,3).
59
60

The largest SBAC was observed in stands dominated by small trees ($d_m < 200$ mm). SBAC decreased rapidly with mean tree diameter up to c. 9800 mm after which it increased again (Figure 2). Considering stand basal area, SBAC increased from low to medium stand basal area values, stabilising from medium to high stand basal area values (Figure 2).

The effect of WAI on SBAC was particularly strong in stands with low mean d.b.h. (Figure 3a) and low basal area (Figure 3b). With increasing minimum temperature, a non-linear relationship with SBAC was observed with a SBAC peak at intermediate temperatures (Figure 4c), but this relationship was strongly affected by mean d.b.h. (Figure 3c) and stand basal area (Figure 3d). The positive effect of increasing minimum temperature on SBAC was particularly strong at high mean d.b.h., showing a more neutral relationship at low mean d.b.h. (Figure 3c). Stands with low basal area showed the lowest SBAC at negative minimum temperatures, and the highest SBAC at high basal area (Figure 3d). Moreover, we observed that the effect of minimum temperature on SBAC was greater in wet areas (WAI positive) than in dry areas (WAI negative) (Figure 4a). SBAC was positively associated with water availability (i.e. WAI) in hot regions (i.e. Figure 4a,b) but no such relationship was found in regions with low minimum temperatures (Figure 4a).

We observed an increase in SBAC with increases in recent temperature anomalies (see positive value of parameter β_9 , Table 3). This positive effect of recent warming on SBAC was particularly strong in stands with low mean d.b.h. (Figure 3e) and high basal area (Figure 3f). The positive effect of recent temperature increase on SBAC was also particularly high in wet areas, turning to neutral in dry sites (Figure 4b). The positive effect of recent temperature increase was observed along the full length of the minimum temperature gradient and was particularly strong at low minimum

temperatures (Figure 4c). The negative effects of recent precipitation reductions on SBAC increments were observed in both dry and wet areas, but the positive effects of precipitation increase only occurred in wet areas (i.e. positive WAI, Figure 4d).

DISCUSSION

The plot-based forest inventory information from Spain, Germany and Finland showed that in the late 20th century undisturbed European forests experienced a net increase in stand basal area, in agreement with previous studies (e.g. Ciais and others 2008; Bellassen and others 2011). These increments were particularly large in the temperate biome, turning to neutral or even negative in some areas of the Mediterranean and northern boreal forests. Patterns of stand basal area increase were highly influenced by stand structure (mean d.b.h. and stand basal area) and climate (water availability and minimum temperatures), but also by recent temperature and precipitation anomalies. The largest stand basal area changes (SBAC) occurred in relatively young forests or forests in early development stages (i.e. low mean d.b.h. and low-medium basal area) in mesic environments (i.e. not constrained by water or energy availability). Together, these results suggest that the carbon sink potential of European forests could be strongly constrained in water-limited Mediterranean forests, where the positive effects of recent climate warming may be offset by competition and climatic stress.

Patterns of stand basal area change and its components

All three biomes showed a net increase in stand basal area, in agreement with previous studies that have reported a general increase in biomass in the second half of the 20th century (Kauppi and others 1992; Ciais and others 2008; Bellassen and others 2011; Pan and others 2011). The positive correlation between stand basal area change (SBAC) and growth suggests that factors controlling tree growth, such as stand structure, climate and

recent climatic anomalies are fundamental drivers of SBAC (Gómez-Aparicio and others 2011; Vayreda and others 2012). However, we observed a negative correlation between SBAC and stand loss suggesting that stochastic mortality processes may have a key role in the future on aboveground productivity and forest structure, particularly under climate change (Allen and others 2010; Benito-Garzón and others 2013; Ruiz-Benito and others 2013). These results suggest that both growth and mortality could potentially affect species performance and future species distribution (Benito-Garzón and others 2013).

The temperate biome had the highest SBAC increments, which agrees with global analyses of the aboveground forest carbon sink (Pan and others 2013). The largest SBAC increments in temperate forest are probably due to increased tree growth in parts of the latitudinal gradient not strongly limited by temperature or water availability (e.g. Gerten and others 2008). It has been suggested that temperature controls tree growth in boreal forests, whereas moisture and water availability are key drivers in central and southern Europe (e.g. Vayreda and others 2012; Babst and others 2013). The highest mortality rates were observed in the Spanish part of the temperate biome, probably due to the fact that the Iberian Peninsula harbours the southern distribution limit of several widespread European species (Hewitt 2000; Hampe and Petit 2005). In high-density Iberian forests increased temperature and drought events have been related to tree mortality and forest decline (e.g. Carnicer and others 2011; Sánchez-Salguero and others 2012; Ruiz-Benito and others 2013), most likely due to an increase in tree density resulting from a reduction in management practices throughout the Iberian Peninsula (e.g. Madrigal 1998; Ruiz-Benito and others 2012). Moreover, most data from the Iberian Peninsula covers the early 21th century coinciding with the

1
2
3
4
5
6
7
8
9
10
11
12
13
14
15
16
17
18
19
20
21
22
23
24
25
26
27
28
29
30
31
32
33
34
35
36
37
38
39
40
41
42
43
44
45
46
47
48
49
50
51
52
53
54
55
56
57
58
59
60

366 severe drought of the 2000s (see Table S1), of which the effects on European forest
367 primary productivity have already been reported (Ciais and others 2005).

368 **Structural and climatic factors determining stand basal area change**

369 Mean d.b.h. was the variable with the highest overall effect on basal area change,
370 followed by water availability and stand basal area (Table 2). Mean d.b.h. and stand
371 basal area are both related to stand age, and reflect past disturbances (e.g. fire or logging
372 history). Our results are consistent with other studies that found that structural variables
373 are particularly important in driving biomass changes, and thus growth and mortality
374 processes (e.g. Vilá-Cabrera and others 2011; Vayreda and others 2012). Stand age has
375 been shown to be particularly important in the net ecosystem productivity of different
376 forest types including boreal and temperate broadleaved forests (Magnani and others
377 2007).

378 The high SBAC observed at medium stand basal area and low mean d.b.h. (see
379 Figure 2 and supplementary Figure S1 and S2) suggests that European forests could be
380 in competitive thinning stages and that they will continue to act as carbon sinks in the
381 near future (Ciais and others 2008; Vayreda and others 2012). The form of the
382 relationship between SBAC and stand basal area is similar to the well-known pattern for
383 above-ground biomass increment, which often increases with stand basal area then
384 levels off at higher population densities (e.g. Charru and others 2010; McMahon and
385 others 2010). Our results agree with typical forest development, where relatively young
386 stands accumulate carbon (i.e. in developing stages), but biomass increments start to
387 decline when the stands are at high competitive levels (i.e. intermediate mean d.b.h. and
388 high stand basal area, Coomes and Allen 2007).

Water availability had a strong, linear influence on SBAC (Table 2, Figure 3a,b), emphasising the central role that heat and water stress have in driving growth and mortality and, thus, are fundamental factors of carbon balance (Magnani and others 2007; Charruand others 2010). The positive effect of water availability on SBAC was particularly pronounced in relatively young forest (i.e. low mean d.b.h. and low stand basal area) and in hot areas (i.e. high minimum temperatures). Although differential sensitivity in tree growth and tree mortality with age have been reported, greater sensitivities have been found in either young trees (e.g. Suarez and others 2004; Vieira and others 2009) or older trees (possibly related to hydraulic limitation, see Carrer and Urbinati 2004). Our results suggest that relatively young forests or forests in developing stages are particularly sensitive to low water availability and temperature-related stress (see Coll and others 2013; [Madrigal-González and Zavala 2014](#)).

The relationship between SBAC and the minimum temperature gradient reflects the large gradient covered from cold boreal to warm Mediterranean forests (see Figure 3c,d), which is a primary factor influencing tree species distributions (Woodward and Williams 1987). Moreover, we observed that minimum temperatures had a positive correlation with SBAC in forests with high mean d.b.h., low stand basal area or positive water availability (Figure 3c,d and Figure 4a, respectively). This result suggests that minimum temperature could be an important factor limiting primary productivity in northern European forests (i.e. WAI positive and minimum temperature lower than -8 °C, see supplementary Figure S1), but in southern dry forests water availability is the main constraint (Boisvenue and Running 2006).

Effect of recent temperature and precipitation anomalies on stand basal area change

1
2
3 413 Recent climate change has had a profound impact on SBAc. Increases in temperature
4
5 414 and precipitation were associated with increased SBAc (Figure 3e-g), and although its
6
7
8 415 effect was lower than those of stand structure or mean climate, we observed significant
9
10 416 interactive effects (Fig 3,4). Vayreda and others (2012) found that recent shifts in
11
12 417 climate had important effects on biomass growth in Spanish forests, and reported that
13
14
15 418 this effect had less influence on growth than stand structure or spatial climatic
16
17
18 419 variability. Sala and others (2012) have also suggested that productivity is more affected
19
20 420 by spatial than temporal variation in climate.

21
22 421 The general positive effect of increased temperature on basal area increments
23
24 422 observed in wet areas, agrees with other studies that have reported this effect when
25
26
27 423 water is not a limiting factor (McMahon and others 2010; Vayreda and others 2012).
28
29 424 Thus, warming could particularly enhance plant growth in boreal and temperate
30
31 425 European forests because of increases in metabolic rates (Anderson and others 2006;
32
33
34 426 Way and Oren, 2010) or longer growing seasons (Myneni and others 1991). In our
35
36 427 study, the trend for increased SBAc with increasing recent temperatures was observed
37
38
39 428 in relatively young forests, which are likely to be in a growth peak (Gómez-Aparicio
40
41 429 and others 2011). Overall, these results suggest that the positive effects of warming on
42
43 430 SBAc could vary greatly, depending on climate and stand structure. Thus stand basal
44
45
46 431 area increments could potentially be neutralised in water-limited forests, such as those
47
48
49 432 found in Mediterranean regions (see also Vayreda and others 2012), and in mature
50
51 433 forests where growth is generally less than forests in competitive thinning stages if there
52
53 434 is a slow filling of canopy gaps, or water or nutrient limitation (Coomes and others
54
55 435 2012).

56
57
58 436 Although the effect of recent shifts in precipitation on SBAc was much smaller
59
60 437 than the effect of increasing temperatures (Table 2), the relatively small SBAc in areas

with reduced precipitation was maintained along the entire water availability gradient (Figure 4d), but was particularly important in wet areas (i.e. temperate and boreal biomes). This result suggests that although drought stress could cause reduced growth (Barber and others 2000; Silva and others 2010) rainfall shortage could also cause important decreases in productivity (Ciais and others 2005). This could be particularly severe in wet compared to dry areas, probably due to the poor adaptation of plants to water shortages in these regions (Vicente-Serrano and others 2013). Nevertheless, in dry sites, such as water-limited Mediterranean forests, temporal increases in precipitation correlated with increases in SBAC (Figure 4d). This result suggests that water-limited areas can be expected to respond to any increasing precipitation with large biomass increments (e.g. Knapp and Smith 2001; Gerten and others 2008).

Implications for stand basal area change in European forests

This work provides support for the view that stand structure and climatic heterogeneity are critical drivers of stand basal area change. These drivers should be taken into account when determining the potential carbon sink or source of European forests over time across biomes, because limiting factors and possible trends may radically differ depending on climatic and structural conditions.

We observed a high net annual increment in recent stand basal area change of 0.43 m² ha⁻¹ yr⁻¹, mainly due to stand basal area gains (c. 3.8%) and partially constrained by stand basal area losses due to mortality (c. 0.06%, Table 1). A large fraction of European forests are undergoing post-disturbance secondary succession (including management practices)~~European forests are recovering from disturbances and are undergoing management~~, which could be an explanation for the sink role observed during the 1990s (e.g. Schimel and others 2001). Despite of the relatively high

increase in stand basal area in the period considered in this study, we observed a high variability in the response. Our results suggest that the changes in basal area are highly influenced by interactive effects between stand structure, climate and climate warming.

The repeated inventory-based measures used in this study highlight the potential role of forests in accumulating biomass, but our results suggest that current stand structure (i.e. the relatively young age and high density of European forests) and the potential effects of spatial and temporal variations in climate could constrain biomass increases in the absence of disturbances or other management actions (e.g. fire or extensive management were not explicitly considered in this study). On the one hand, we observed that relatively young forests or forests in competitive thinning stages have a greater potential to act as aboveground carbon sinks than mature forest (e.g. Luyssaert and others 2010; Pan and others 2011), however large areas of European forests are increasing in density which may result in biomass increments levelling off (e.g. Charru and others 2010). In addition, the largest increments in stand basal area were observed in forests least limited by water or temperature, and the carbon sink role of European forests could be strongly modulated by climate change. Stand basal area change could be caused by either reduced forest growth or increased tree mortality, and thus may affect species distributions (Benito-Garzón and others 2013). Moreover, rapid climate warming may cause large-scale dieback in some forests (e.g. Allen and others 2010), increased mortality or reduced growth caused by interactions between climate and stand structure (e.g. Gómez-Aparicio and others 2011; Ruiz-Benito and others 2013).

Limitations in water and/or energy availability are fundamental drivers constraining biomass increment (e.g. Boisvenue and Running 2006), as demonstrated by the fact that Mediterranean (dry areas limited by water availability) and northern boreal forests (limited by minimum temperature) had the lowest SBAC increments. Biomass

increments in Mediterranean water-limited forests have been relatively less affected by recent climate warming compared to stands in temperate and boreal biomes (i.e. see reduced SBAC response to increased temperature, Fig. 4b). However, basal area accumulation due to the positive effects of climate warming is unlikely to continue at its current rate in regions where precipitation is declining and forests are ageing. Early signs of carbon sink saturation have been observed in European forests (Narbuurs and others 2013), congruent with our results because aboveground biomass increments are strongly dependent on current forest structure (see also Vayreda and others 2012). However, our results may overestimate the rate of aboveground basal area accumulation in European forests because we deliberately excluded harvested plots from our analyses, in which stand basal area could have dropped substantially. Overall, we suggest that forests in developing stages constitute an important short-term aboveground carbon sink, but these forests could be particularly vulnerable to climate stress and competition, especially in the water-limited Mediterranean region.

ACKNOWLEDGEMENTS

This research was supported by the CARBO-Extreme (FP7-ENV-2008-1-226701) and Leverhulme Trust project IN-2013-004. PRB was supported by a FPU fellowship (AP2008-01325). We thank A. Herrero for interesting discussion on earlier versions of this manuscript, the MAGRAMA for granting access to the Spanish Forest Inventory data, the Johann Heinrich von Thünen-Institut for making data from the first and second German National Forest Inventory available, and to the Finnish Forest Research Institute (METLA) for making permanent sample plot data from 1985-86 and from 1995 available. We also acknowledge access to UDel_AirT_Precip data provided by the NOAA/OAR/ESRL PSD, Boulder, Colorado, USA (<http://www.esrl.noaa.gov/psd/>).

511 REFERENCES

512 Allen CD, Macalady AK, Chenchouni H, Bachelet D, McDowell N, Vennetier M,
513 Kitzberger T, Rigling A, Breshears DD, Hogg EH, Gonzalez P, Fensham R, Zhang
514 Z, Castro J, Demidova N, Lim J-H, Allard G, Running SW, Semerci A, Cobb N.
515 2010. A global overview of drought and heat-induced tree mortality reveals
516 emerging climate change risks for forests. *Forest Ecology and Management* 259:
517 660-684.

518 Anderson KJ, Allen AP, Gillooly JF, Brown JH. 2006. Temperature-dependence of
519 biomass accumulation rates during secondary succession. *Ecology Letters* 9: 673-
520 682.

521 Babst F, Poulter B, Trouet V, Tan K, Neuwirth B, Wilson R, Carrer M, Grabner M,
522 Tegel W, Levanic T, Panayotov M, Urbinati C, Bouriaud O, Ciais P, Frank
523 D. 2013. Site- and species-specific responses of forest growth to climate across the
524 European continent. *Global Ecology and Biogeography* 22: 706-717.

525 Barber VA, Juday GP, Finney BP. 2000. Reduced growth of Alaskan white spruce
526 in the twentieth century from temperature-induced drought stress. *Nature* 405: 668-
527 673.

528 Bates D, Maechler M, Bolker B. 2012. lme4: Linear mixed-effects models using Eigen
529 and Eigen R. R package version 0.999375-42. <http://lme4.r-forge.r-project.org/>.

530 Bellassen V, Luyssaert S (2014) Carbon sequestration: Managing forest in uncertain
531 times. *Nature* 506: 153-155.

532 Bellassen V, Viovy N, Luyssaert S, Le Maire G, Schelhaas MJ, Ciais P. 2011.
533 Reconstruction and attribution of the carbon sink of European forests between 1950
534 and 2000. *Global Change Biology* 17: 3274-3292.

535 Belsey DA. 1991. Conditioning diagnostics, collinearity and weak data in
536 regression. New York: Wiley.

537 Bolker BM, Brooks ME, Clark CJ, Geange SW, Poulsen JR, Stevens MHH, White
538 J-SS. 2009. Generalized linear mixed models: a practical guide for ecology and
539 evolution. *Trends in Ecology & Evolution* 24: 127-135.

540 Benito-Garzón M, Ruiz-Benito P, Zavala MA. 2013. Inter-specific differences in
541 tree growth and mortality responses to climate determine potential species
542 distribution limits in Iberian forests. *Global Ecology and Biogeography* 22: 1141-
543 1151.

544 Boisvenue C, Running SW. 2006. Impacts of climate change on natural forest
545 productivity – evidence since the middle of the 20th century. *Global Change Biology*
546 12: 862-882.

- 547 Burnham KP, Anderson DR. 2002. Model Selection and Multi model Inference: A
548 Practical Information-theoretic Approach. New York: Springer-Verlag New York.
549 488p.
- 550 Cao M, Woodward FI. 1998. Dynamic responses of terrestrial ecosystem carbon
551 cycling to global climate change. *Nature* 393: 249-252.
- 552 Canadell JG, Raupach MR. 2008. Managing forests for climate change mitigation.
553 *Science* 320: 1456-1457.
- 554 Carrer M, Urbinati C. 2004. Age-dependent tree-ring growth responses to climate in
555 *Larix decidua* and *Pinus cembra*. *Ecology* 85: 730-740.
- 556 Carnicer J, Coll M, Ninyerola M, Pons X, Sánchez G, Peñuelas J. 2011. Widespread
557 crown condition decline, food web disruption, and amplified tree mortality with
558 increased climate change-type drought. *Proceedings of the National Academy of*
559 *Sciences* 108: 1474-1478.
- 560 Charru M, Seynave I, Morneau F, Bontemps JD. 2010. Recent changes in forest
561 productivity: An analysis of national forest inventory data for common beech
562 (*Fagus sylvatica* L.) in north-eastern France. *Forest Ecology and Management* 260:
563 864-874.
- 564 Christensen JH, Hewitson B, Busuioc A, Chen A, Gao X, Held I, Jones R, Kolli RK,
565 Kwon WT, Laprise R, Magaña Rueda V, Mearns L, Menéndez CG, Räisänen J,
566 Rinke A, Sarr A, Whetton P. 2007. Regional climate projections. Solomon S, Qin D,
567 Manning M, Chen Z, Marquis M, Averyt KB, Tignor M, Miller HL, editors.
568 *Climate change 2007: The physical science basis*. Cambridge: University Press.
569 p847-943.
- 570 Ciais P, Reichstein M, Viovy N, Granier A, Ogee J, Allard V, Aubinet M,
571 Buchmann N, Bernhofer C, Carrara A, Chevallier F, De Noblet N, Friend AD,
572 Friedlingstein P, Grunwald T, Heinesch B, Keronen P, Knohl A, Krinner G, Loustau
573 D, Manca G, Matteucci G, Miglietta F, Ourcival JM, Papale D, Pilegaard K, Rambal
574 S, Seufert G, Soussana JF, Sanz MJ, Schulze ED, Vesala T, Valentini R. 2005.
575 Europe-wide reduction in primary productivity caused by the heat and drought in
576 2003. *Nature* 437: 529-533.
- 577 Ciais P, Schelhaas MJ, Zaehle S, Piao SL, Cescatti A, Liski J, Luyssaert S, Le-Maire
578 G, Schulze E-D, Bouriaud O, Freibauer A, Valentini R, Nabuurs GJ. 2008. Carbon
579 accumulation in European forests. *Nature Geosciences* 1: 425-429.
- 580 Coll M, Peñuelas J, Ninyerola M, Pons X, Carnicer J. 2013. Multivariate effect
581 gradients driving forest demographic responses in the Iberian Peninsula. *Forest*
582 *Ecology and Management* 303: 195-209.

1
2
3 583 Coomes DA, Allen RB. 2007. Effects of size, competition and altitude on tree
4 584 growth. *Journal of Ecology* 95: 1084-1097.
5
6
7 585 Coomes DA, Holdaway RJ, Kobe RK, Lines ER, Allen RB. 2012. A general
8 586 integrative framework for modelling woody biomass production and carbon
9 587 sequestration rates in forests. *Journal of Ecology* 100: 42-64.
10
11
12 588 Dietze MC, Moorcroft PR. 2011. Tree mortality in the eastern and central United
13 589 States: patterns and drivers. *Global Change Biology* 17: 3312-3326.
14
15
16 590 Dixon RK, Solomon AM, Brown S, Houghton RA, Trexler MC, Wisniewski J.
17 591 1994. Carbon pools and flux of global forest ecosystems. *Science* 263: 185-190.
18
19
20 592 Food and Agriculture Organization of the United Nations. 2010. Global Forest
21 593 Resources Assessment 2010. <http://www.fao.org/forestry/fra/fra2010/en/>
22
23
24 594 Gamfeldt L, Snäll T, Bagchi R, Jonsson M, Gustafsson L, Kjellander P, Ruiz-Jaen
25 595 MC, Froberg M, Stendahl J, Philipson CD, Mikusinski G, Andersson E, Westerlund
26 596 B, Andren H, Moberg F, Moen J, Bengtsson J. 2013. Higher levels of multiple
27 597 ecosystem services are found in forests with more tree species. *Nature*
28 598 *Communications* 4: 1340.
29
30
31 599 García-Valdés R, Zavala MA, Araújo MB, Purves DW. 2013. Chasing a moving
32 600 target: projecting climate change-induced changes in non-equilibrium tree species
33 601 distributions. *Journal of Ecology* 101: 441-453.
34
35
36 602 Gerten D, Luo Y, Le Maire G, Parton WJ, Keough C, Weng E, Beier C, Ciais P,
37 603 Cramer W, Dukes JS, Hanson PJ, Knapp AAK, Linder S, Nepstad DAN, Rustad L,
38 604 Sowerby A. 2008. Modelled effects of precipitation on ecosystem carbon and water
39 605 dynamics in different climatic zones. *Global Change Biology* 14: 2365-2379.
40
41
42 606 Gómez-Aparicio L, García-Valdés R, Ruiz-Benito P, Zavala MA. 2011.
43 607 Disentangling the relative importance of climate, size and competition on tree
44 608 growth in Iberian forests: implications for management under global change. *Global*
45 609 *Change Biology* 17: 2400-2414.
46
47
48
49 610 Goodale CL, Apps MJ, Birdsey RA, Field CB, Heath LS, Houghton RA, Jenkins
50 611 JC, Kohlmaier GH, Kurz W, Liu S, Nabuurs G-J, Nilsson S, Shvidenko AZ. 2002.
51 612 Forest carbon sinks in the northern hemisphere. *Ecological Applications* 12: 891-
52 613 899.
53
54
55 614 Hampe A, Petit RJ. 2005. Conserving biodiversity under climate change: the rear
56 615 edge matters. *Ecology Letters* 8: 461-467.
57
58
59 616 Hember RA, Kurz WA, Metsaranta JM, Black TA, Guy RD, Coops NC. 2012.
60 617 Accelerating regrowth of temperate-maritime forests due to environmental change.
618 618 *Global Change Biology* 18: 2026-2040.

- 619 Hewitt G. 2000. The genetic legacy of the Quaternary ice ages. *Nature* 405: 907-
620 913.
- 621 Hijmans RJ, Cameron SE, Parra JL, Jones PG, Jarvis A. 2005. Very high resolution
622 interpolated climate surfaces for global land areas. *International Journal of*
623 *Climatology* 25: 1965-1978.
- 624 Hilborn R, Mangel M. 1997. *The ecological detective: confronting models with*
625 *data*. Princeton (NJ): Princeton University Press.
- 626 Hoch G, Körner C. 2012. Global patterns of mobile carbon stores in trees at the
627 high-elevation tree line. *Global Ecology and Biogeography* 21: 861-871.
- 628 Lines ER, Zavala MA, Purves DW, Coomes DA. 2012. Predictable changes in
629 aboveground allometry of trees along gradients of temperature, aridity and
630 competition. *Global Ecology and Biogeography* 21: 1017-1028.
- 631 Kauppi PE, Mielikäinen K, Kuusela K. 1992. Biomass and carbon budget of
632 European forests, 1971 to 1990. *Science* 256: 70-74.
- 633 Knapp AK, Smith MD. 2001. Variation among biomes in temporal dynamics of
634 aboveground primary production. *Science* 291: 481-484.
- 635 Kunstler G, Albert CH, Courbaud B, Lavergne S, Thuiller W, Vieilledent G,
636 Zimmermann NE, Coomes DA. 2011. Effects of competition on tree radial-growth
637 vary in importance but not in intensity along climatic gradients. *Journal of Ecology*
638 99: 300-312.
- 639 Luo Y, Gerten D, Le Maire G, Parton WJ, Weng E, Zhou X, Keough C, Beier C,
640 Ciais P, Cramer W, Dukes JS, Emmett B, Hanson PJ, Knapp A, Linder S, Nepstad
641 DAN, Rustad L. 2008. Modeled interactive effects of precipitation, temperature, and
642 [CO₂] on ecosystem carbon and water dynamics in different climatic zones. *Global*
643 *Change Biology* 14: 1986-1999.
- 644 Luyssaert S, Ciais P, Piao SL, Schulze ED, Jung M, Zaehle S, Schelhaas MJ,
645 Reichstein M, Churkina G, Papale D, Abril G, Beer C, Grace J, Loustau D,
646 Matteucci G, Magnani F, Nabuurs GJ, Verbeeck H, Sulkava M, Van Der Werf GR,
647 Janssens IA. 2010. The European carbon balance. Part 3: Forests. *Global Change*
648 *Biology* 16: 1429-1450.
- 649 Madrigal A. 1998. Problemática de la ordenación de masas artificiales en España.
650 *Cuadernos de la Sociedad Española de Ciencias Forestales* 6: 13-20.
- 651 Magnani F, Mencuccini M, Borghetti M, Berbigier P, Berninger F, Delzon S,
652 Grelle A, Hari P, Jarvis PG, Kolari P, Kowalski AS, Lankreijer H, Law BE,
653 Lindroth A, Loustau D, Manca G, Moncrieff JB, Rayment M, Tedeschi V, Valentini

1
2
3 654 R, Grace J. 2007. The human footprint in the carbon cycle of temperate and boreal
4 655 forests. *Nature* 447: 849-851.
5
6
7 656 Madrigal-González J, Zavala MA. 2014. Competition and tree age modulated last
8 657 century pine growth responses to high frequency of dry years in a water limited
9 658 forest ecosystem. *Agricultural and Forest Meteorology* 192-193: 18-26.
10
11
12 659 McMahon SM, Parker GG, Miller DR. 2010. Evidence for a recent increase in forest
13 660 growth. *Proceedings of the National Academy of Sciences* 107: 3611-3615.
14
15
16 661 Millennium Ecosystem Assessment. 2005. Ecosystem and human well-being:
17 662 biodiversity synthesis. Washington, DC: Island Press.
18
19
20 663 Myneni RB, Keeling CD, Tucker CJ, Asrar G, Nemani RR. 1991. Increased plant
21 664 growth in the northern high latitudes from 1981 to 1991. *Nature* 386: 698-702.
22
23
24 665 Nabuurs GJ, Lindner M, Verkerk PJ, Gunia K, Deda P, Michalak R, Grassi G. 2013.
25 666 First signs of carbon sink saturation in European forest biomass. *Nature Climate*
26 667 *Change* 3: 792-796.
27
28
29 668 Nabuurs GJ, Schelhaas MJ, Mohren GMJ, Field CB. 2003. Temporal evolution of
30 669 the European forest sector carbon sink from 1950 to 1999. *Global Change Biology*
31 670 9: 152-160.
32
33
34 671 Nakagawa S, Schielzeth H. 2013. A general and simple method for obtaining R^2
35 672 from generalized linear mixed-effects models. *Methods in Ecology and Evolution* 4:
36 673 133-142.
37
38
39 674 Oksanen J, Blanchet FG, Kindt R;Legendre P, O'Hara RG, Simpson GL, Solymos P,
40 675 Stevens M, Wagner H. 2010. Multivariate analysis of ecological communities in R:
41 676 vegan tutorial. R package version 1.17-0. [http://CRAN.R-](http://CRAN.R-project.org/package=vegan)
42 677 [project.org/package=vegan](http://CRAN.R-project.org/package=vegan).
43
44
45 678 Olson DM, Dinerstein E, Wikramanayake ED, Burgess ND, Powell GVN,
46 679 Underwood EC, D'amico JA, Itoua I, Strand HE, Morrison JC, Loucks CJ, Allnutt
47 680 TF, Ricketts TH, Kura Y, Lamoreux JF, Wettengel WW, Hedao P, Kassem KR.
48 681 2001. Terrestrial ecoregions of the world: a new map of life on earth. *Bioscience* 51:
49 682 933-938.
50
51
52
53 683 Pan Y, Birdsey RA, Fang J,Houghton R, Kauppi PE, Kurz WA, Phillips OL,
54 684 Shvidenko A, Lewis SL, Canadell JG, Ciais P, Jackson RB, Pacala SW, McGuire
55 685 AD, Piao S, Rautiainen A, Sitch S, Hayes D. 2011. A large and persistent carbon
56 686 sink in the world's forests. *Science* 333: 988-993.
57
58
59 687 Pastor J, Post WM (1988) Response of northern forests to CO₂-induced climate
60 688 change. *Nature* 334: 55-58.

- Peng J, Dan L, Huang M. 2014. Sensitivity of global and regional terrestrial carbon storage to the direct CO₂ effect and climate change based on the CMIP5 model intercomparison. *PLoS ONE* 9: e95282.
- Pinheiro JC, Bates DM. 2000. Mixed effect models in S and S-Plus. New York: Springer-Verlag New York. 528 p.
- R Development Core Team. 2012. R: a language and environment for statistical computing. Vienna: R Foundation for Statistical Computing. www.r-project.org.
- Ruiz-Benito P, Gómez-Aparicio L, Zavala MA. 2012. Large scale assessment of regeneration and diversity in Mediterranean planted pine forests along ecological gradients. *Diversity and Distributions* 18: 1092–1106.
- Ruiz-Benito P, Lines ER, Gómez-Aparicio L, Zavala MA, Coomes DA. 2013. Patterns and drivers of tree mortality in Iberian forests: climatic effects are modified by competition. *PLoS ONE* 8: e56843.
- Sala OE, Gherardi LA, Reichmann L, Jobbágy E, Peters D. 2012. Legacies of precipitation fluctuations on primary production: theory and data synthesis. *Philosophical Transactions of the Royal Society B: Biological Sciences* 367: 3135–3144.
- Sánchez-Salguero R, Navarro-Cerrillo R, Camarero J, Fernández-Cancio Á. 2012. Selective drought-induced decline of pine species in southeastern Spain. *Climatic Change* 113: 767–785.
- Schimel D. 2007. Carbon cycle conundrums. *Proceedings of the National Academy of Sciences* 104: 18353–18354.
- Schimel DS, House JI, Hibbard KA, Bousquet P, Ciais P, Peylin P, Braswell BH, Apps MJ, Baker D, Bondeau A, Canadell J, Churkina G, Cramer W, Denning AS, Field CB, Friedlingstein P, Goodale C, Heimann M, Houghton RA, Melillo JM, Moore B, Murdiyarso D, Noble I, Pacala SW, Prentice IC, Raupach MR, Rayner PJ, Scholes RJ, Steffen WL, Wirth C. 2001. Recent patterns and mechanisms of carbon exchange by terrestrial ecosystems. *Nature* 414: 169–172.
- Sheil D, Burslem DFRP, Alder D. 1995. The interpretation and misinterpretation of mortality rate measures. *Journal of Ecology* 83: 331–333.
- Slik JWF, Aiba S-I, Brearley FQ, Cannon CH, Forshed O, Kitayama K, Nagamasu H, Nilus R, Payne J, Paoli G, Poulsen AD, Raes N, Sheil D, Sidiyasa K, Suzuki E, van Valkenburg JLCH. 2010. Environmental correlates of tree biomass, basal area, wood specific gravity and stem density gradients in Borneo's tropical forests. *Global Ecology and Biogeography* 19: 50–60.

1
2
3 724 Silva LCR, Anand M, Leithead MD. 2010. Recent widespread tree growth decline
4 725 despite increasing atmospheric CO₂. PLoS ONE 5: e11543.
5
6
7 726 Suarez ML, Ghermandi L, Kitzberger T. 2004. Factors predisposing episodic
8 727 drought-induced tree mortality in *Nothofagus*– site, climatic sensitivity and growth
9 728 trends. Journal of Ecology 92: 954-966.
10
11
12 729 Spiecker H. 1999. Overview of recent growth trends in European forests. Water,
13 730 Air, & Soil Pollution 116: 33-46.
14
15
16 731 Sykes M, Prentice IC. 1996. Climate change, tree species distributions and forest
17 732 dynamics: A case study in the mixed conifer/northern hardwoods zone of Northern
18 733 Europe. Climatic Change 34: 161-177.
19
20
21 734 Valentini R, Matteucci G, Dolman AJ, Schulze E-D, Rebmann C, Moors EJ,
22 735 Granier A, Gross P, Jensen NO, Pilegaard K, Lindroth A, Grelle A, Bernhofer C,
23 736 Grunwald T, Aubinet M, Ceulemans R, Kowalski AS, Vesala T, Rannik U,
24 737 Berbigier P, Loustau D, Gu[eth]mundsson J, Thorgeirsson H, Ibrom A, Morgenstern
25 738 K, Clement R, Moncrieff J, Montagnani L, Minerbi S, Jarvis PG. 2000. Respiration
26 739 as the main determinant of carbon balance in European forests. Nature 404: 861-
27 740 865.
28
29
30
31 741 vanMantgem PJ, Stephenson NL, Byrne JC, Daniels LD, Franklin JF, Fule PZ,
32 742 Harmon ME, Larson AJ, Smith JM, Taylor AH, Veblen TT.2009. Widespread
33 743 increase of tree mortality rates in the western United States. Science 323: 521-524.
34
35
36 744 Vayreda J, Martínez-Vilalta J, Gracia M, Retana J. 2012. Recent climate changes
37 745 interact with stand structure and management to determine changes in tree carbon
38 746 stocks in Spanish forests. Global Change Biology 18: 1028-1041.
39
40
41 747 Vicente-Serrano SM, Gouveia C, Camarero, Beguería S, Trigo R, López-Moreno JI,
42 748 Azorín-Molina Cs, Pasho E, Lorenzo-Lacruz J, Revuelto J, Morán-Tejeda E,
43 749 Sánchez-Lorenzo A. 2013. Response of vegetation to drought time-scales across
44 750 global land biomes. Proceedings of the National Academy of Sciences 110: 52-57.
45
46
47 751 Vieira J, Campelo F, Nabais C. 2009. Age-dependent responses of tree-ring growth
48 752 and intra-annual density fluctuations of *Pinus pinaster* to Mediterranean climate.
49 753 Trees-Structure and Function 23: 257-265.
50
51
52 754 Vilá-Cabrera A, Martínez-Vilalta J, Vayreda J, Retana J. 2011. Structural and
53 755 climatic determinants of demographic rates of Scots pine forests across the Iberian
54 756 Peninsula. Ecological Applications 31: 1162-1172.
55
56
57 757 Vilà M, Carrillo-Gavilán A, Vayreda J, Bugmann H, Fridman J, Grodzki W, Haase
58 758 J, Kunstler G, Schelhaas M, Trasobares A. 2013 Disentangling biodiversity and
59 759 climatic determinants of wood production. PLoS ONE 8: e53530.
60

- Way DA, Oren R. 2010. Differential responses to changes in growth temperature between trees from different functional groups and biomes: a review and synthesis of data. *Tree Physiology* 30: 669-688.
- Woodward FI, Williams BG. 1987. Climate and plant distribution at global and local scales. *Vegetatio* 69: 189-197.
- Zhao M, Running SW. 2010. Drought-induced reduction in global terrestrial net primary production from 2000 through 2009. *Science* 329: 940-943.
- Zomer R, Bossio D, Trabucco A, Yuanjie L, Gupta D, Singh V. 2007. Trees and water: smallholder agroforestry on irrigated lands in Northern India. Colombo: International Water Management Institute.
- Zomer RJ, Trabucco A, Bossio DA, Verchot LV. 2008. Climate change mitigation: A spatial analysis of global land suitability for clean development mechanism afforestation and reforestation. *Agriculture, Ecosystems & Environment* 126: 67-80.
- Zuur AF, Ieno EN, Walker NJ, Saveliev AA, Smith GM. 2009. Mixed effects models and extension in ecology with R. New York: Springer.

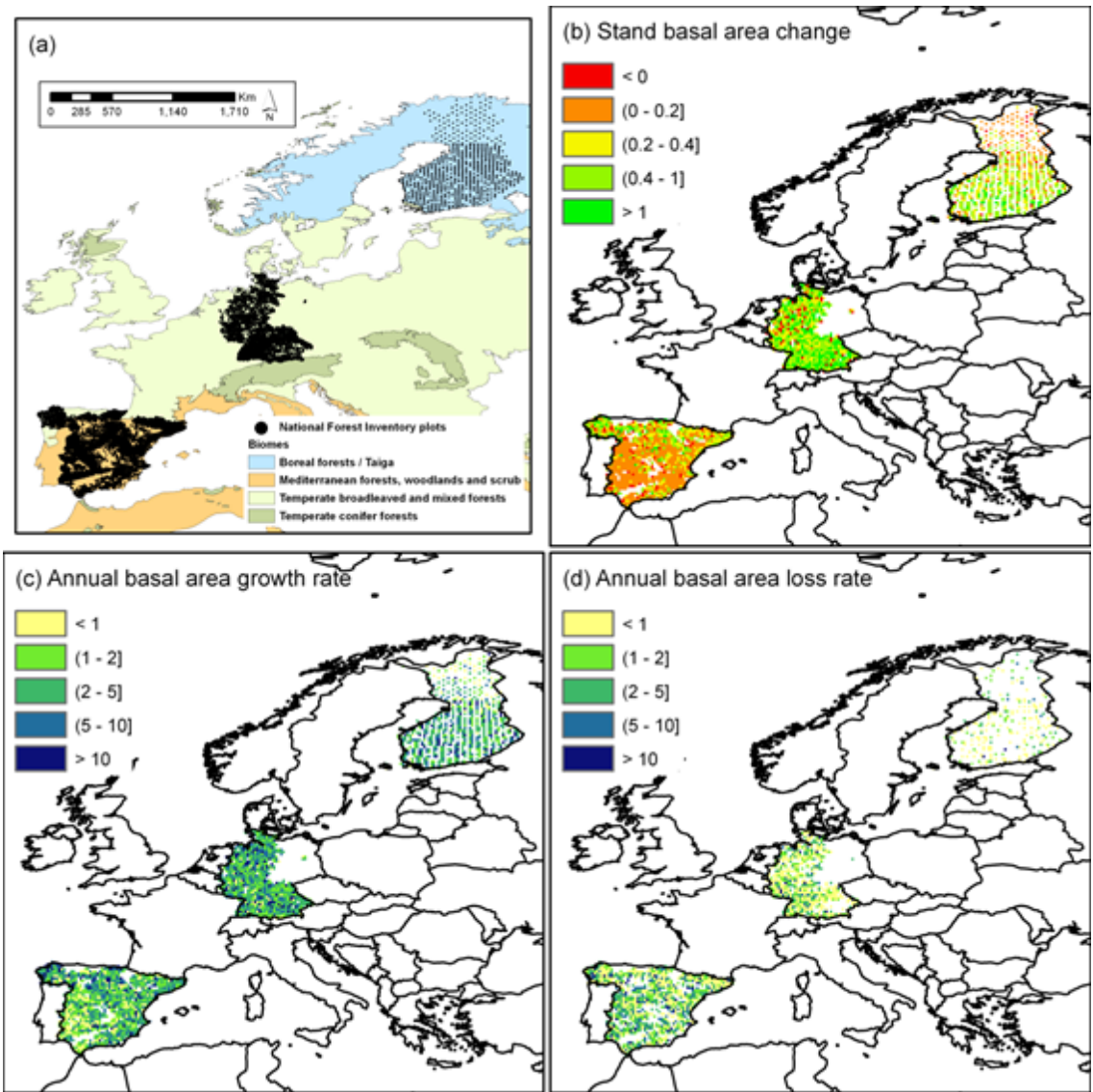


Figure 1.

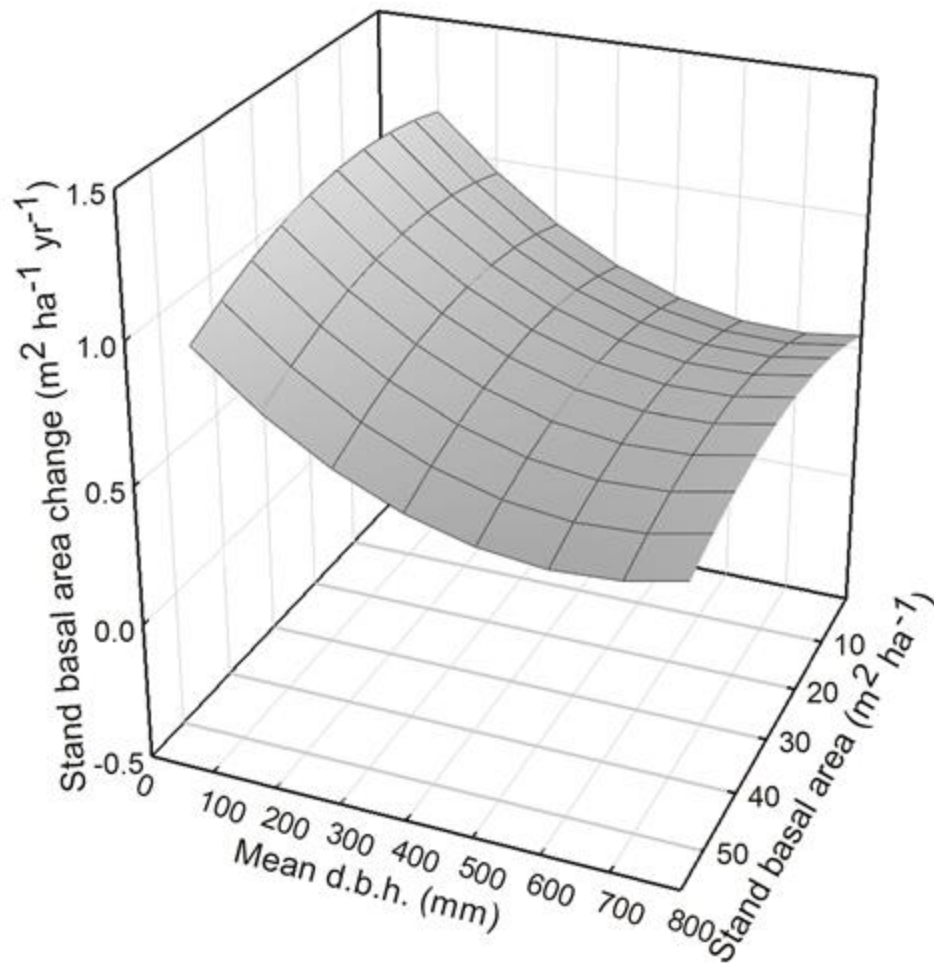


Figure 2.

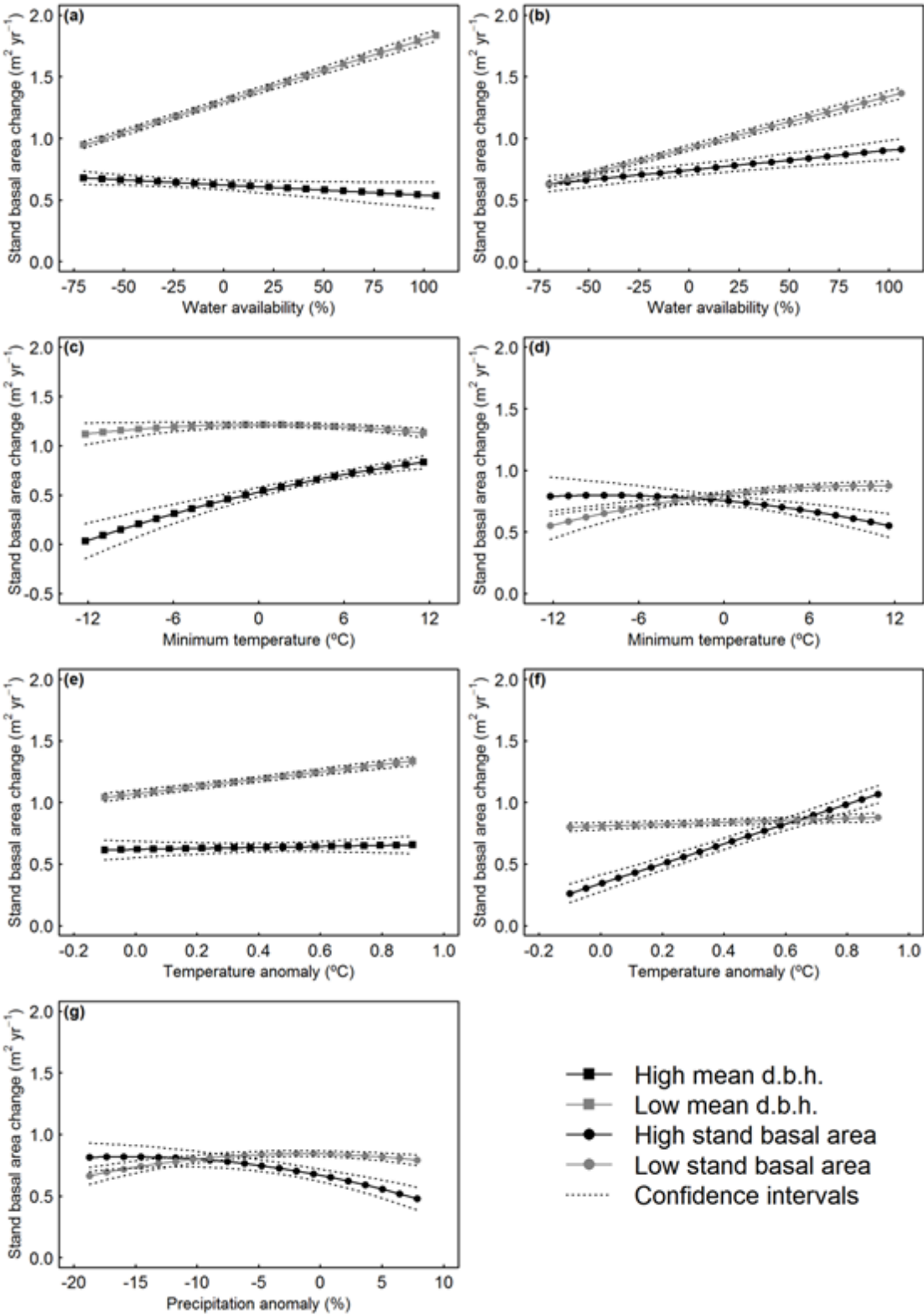


Figure 3.

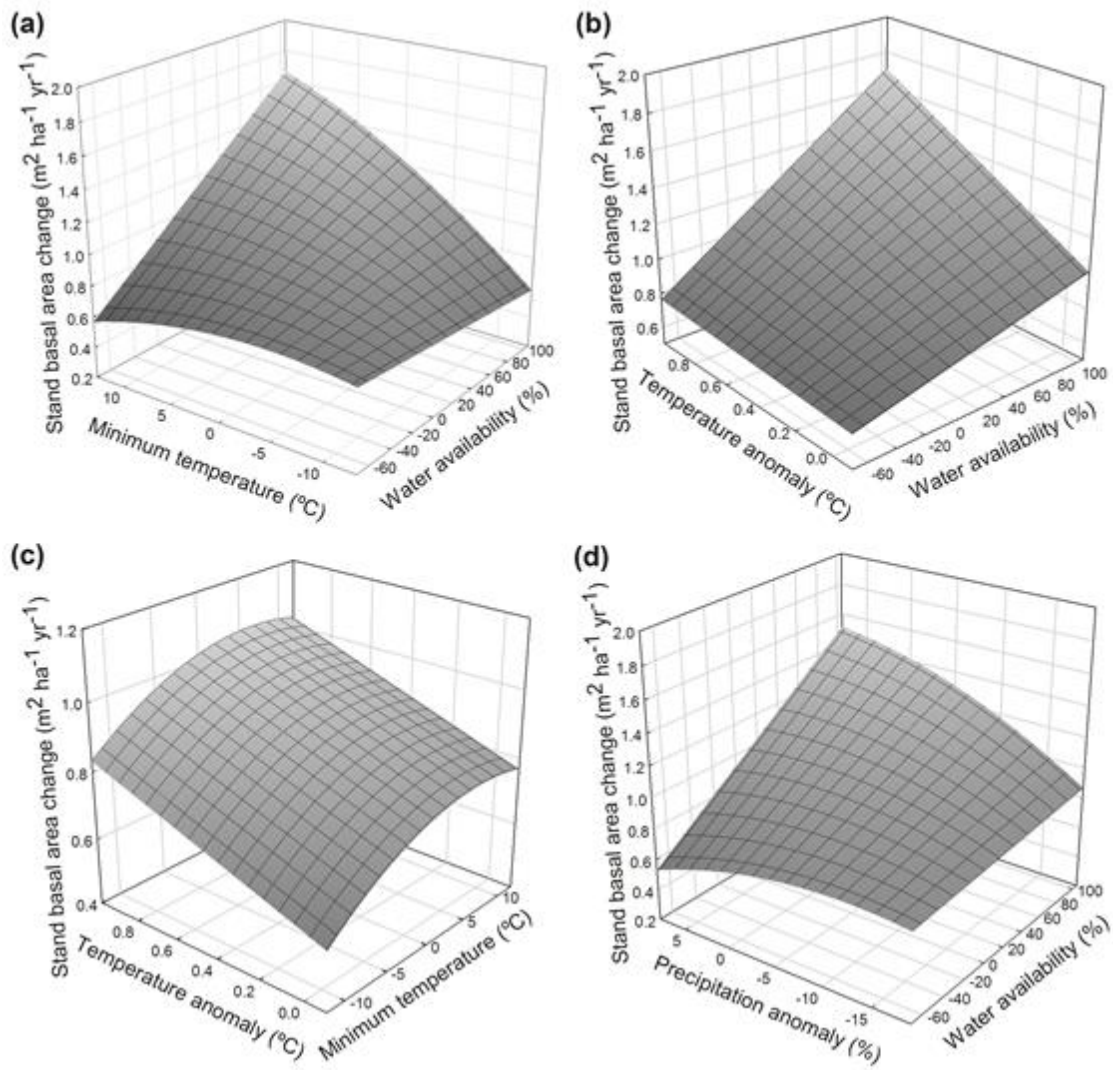


Figure 4.

FIGURE LEGENDS

Figure 1. Map of Spanish, German and Finnish NFI at a spatial resolution of 0.2 x 0.2 degrees: (a) the stands included in this study and the underlying biome distribution (Olson and others 2001), and the spatial distribution of (b) stand basal area change (SBAC, $\text{m}^2 \text{ha}^{-1} \text{yr}^{-1}$), (c) annual basal area growth rate (SBA_{gain} , $\% \text{yr}^{-1}$), (d) annual loss rate (SBA_{loss} , $\% \text{yr}^{-1}$).

Figure 2. Predicted basal area change ($\text{m}^2 \text{ha}^{-1} \text{yr}^{-1}$) by mean d.b.h. (mm) and stand basal area ($\text{m}^2 \text{ha}^{-1}$).

Figure 3. Predicted basal area change in relation to climatic variables in two combinations of mean d.b.h. and basal area. The predicted variation in basal area change ($\text{m}^2 \text{ha}^{-1} \text{yr}^{-1}$, i.e. proxy of biomass change) and 95% confidence intervals were calculated for two combinations of mean d.b.h. (99 percentiles showing high and low d.b.h.) and stand basal area (99 percentiles showing high and low basal area) along: (a,b) water availability (%), (c,d) minimum temperatures, (e,f) temperature anomaly, and (g) precipitation anomaly. The effect of precipitation anomaly on stand basal area change is only shown for combinations of stand basal area, because the interaction between precipitation anomaly and mean d.b.h. did not support a substantial improvement in the model (see Table 2).

Figure 4. Predicted basal area change against main interactions between climatic variables. Tridimensional plot showing the predicted effects on basal area change ($\text{m}^2 \text{ha}^{-1} \text{yr}^{-1}$) of the main interactions: (a) water availability \times minimum temperature, (b) water availability \times temperature anomaly, (c) minimum temperature \times temperature anomaly, and (d) water availability \times precipitation anomaly.

806 **Table 1.** Summary statistics of the inventory plots.

	Mediterranean	Temperate	Boreal	All data
SBA _c (m ² ha ⁻¹ yr ⁻¹)	0.28 ± 0.003 [-0.25, 1.39]	0.71 ± 0.006 [-0.41, 2.43]	0.47 ± 0.009 [-0.05, 1.31]	0.43 ± 0.003 [-0.29, 1.98]
SBA _{gain} (% yr ⁻¹)	3.36 ± 0.046 [0.36, 12.94]	4.59 ± 0.046 [0.71, 20.13]	4.34 ± 4.524 [0.36, 14.00]	3.82 ± 0.021 [0.44, 15.55]
SBA _{loss} (% yr ⁻¹)	0.61 ± 0.013 [0.00, 6.47]	0.63 ± 0.017 [0.00, 5.53]	0.21 ± 0.021 [0.00, 2.06]	0.6 ± 0.000 [0.00, 6.06]
BA (m ² ha ⁻¹)	8.82 ± 0.06 [0.60, 33.43]	21.77 ± 0.12 [1.75, 55.52]	10.1 ± 0.21 [0.34, 29.91]	13.34 ± 0.06 [0.67, 46.17]
d _m (mm)	261.49 ± 0.86 [115.00, 612.60]	284.13 ± 1.06 [113.47, 572.81]	165.25 ± 1.2 [106.83, 284.54]	265.4 ± 0.66 [113.00, 591.92]
WAI (%)	-42.46 ± 0.12 [-67.55, 6.15]	19.77 ± 0.25 [-17.82, 94.48]	15.77 ± 0.21 [0.55, 30.36]	-18.67 ± 0.19 [-65.86, 63.99]
T _{min} (°C)	5.45 ± 0.17 [0.90, 10.60]	1.3 ± 0.24 [-3.00, 8.40]	-9.62 ± 0.56 [-14.60, -5.60]	3.42 ± 0.21 [-8.70, 10.10]
TA (°C)	0.57 ± 0 [0.30, 0.90]	0.32 ± 0 [0.00, 0.70]	0.1 ± 0 [0.00, 0.30]	0.46 ± 0 [0.00, 0.90]
PA (%)	-3.44 ± 0.02 [-9.38, 2.04]	-1.74 ± 0.03 [-7.69, 3.70]	3.73 ± 0.07 [-2.00, 8.89]	-2.56 ± 0.02 [-8.33, 4.08]
No. Plots (%)	61.52%	34.48%	4.00%	100.00%

807 **Table 2.** Alternative models of stand basal area change.

(a) Main and interaction effect models			(b) Main effect models		
	BIC	ΔBIC		BIC	ΔBIC
Full	57946	0	Full	58934	0
No Precipitation anomaly	57959	13	No Precipitation anomaly	58937	3
No Min. temperature	58136	190	No Min. temperature	59018	84
No Temperature anomaly	58229	283	No Temperature anomaly	59085	151
No Stand basal area	58552	606	No Stand basal area	59506	572
No Water availability	59358	1412	No Water availability	60230	1296
No Mean d.b.h.	61285	3339	No Mean d.b.h.	62296	3362
(c) Interaction effect models				BIC	ΔBIC
Full				57946	0
No (Mean d.b.h. × Precipitation anomaly)				57949	3
No (Stand basal area × Mean d.b.h.)				57950	4
No (Mean d.b.h. × Temperature anomaly)				57955	9
No (Stand basal area × Precipitation anomaly)				57963	17
No (Min. temperature × Temperature anomaly)				57964	18
No (Stand basal area × Min. temperature)				57971	25
No (Water availability × Temperature anomaly)				57974	28
No (Stand basal area × Water availability)				57983	37
No (Water availability × Precipitation anomaly)				57984	38
No (Mean d.b.h. × Min. temperature)				57993	47
No (Stand basal area × Temperature anomaly)				58044	98
No (Water availability × Min. temperature)				58053	107
No (Mean d.b.h. × Water availability)				58071	125

808

809

Table 3. Parameters of the final model of stand basal area change.

	Parameter	Mean	SE	LCI	UCI
Intercept	β_1	0.9142	0.0102	0.8960	0.9370
BA	β_2	0.0424	0.0042	0.0348	0.0498
BA ²	β_3	-0.0265	0.0020	-0.0302	-0.0229
d _m	β_4	-0.1983	0.0035	-0.2055	-0.1911
d _m ²	β_5	0.0327	0.0013	0.0296	0.0356
WAI	β_6	0.1371	0.0037	0.1300	0.1442
Tmin	β_7	0.0161	0.0054	0.0064	0.0288
Tmin ²	β_8	-0.0115	0.0035	-0.0183	-0.0043
TA	β_9	0.0505	0.0040	0.0419	0.0603
PA	β_{10}	-0.0090	0.0034	-0.0156	-0.002
PA ²	β_{11}	-0.0075	0.0014	-0.0106	-0.0047
SP	β_{12}	-0.5614	0.0122	-0.5895	-0.5396
FI	β_{13}	-0.5288	0.0371	-0.5965	-0.447
BA × d _m	β_{14}	0.0065	0.0029	0.0009	0.0123
WAI × Tmin	β_{15}	0.0435	0.0042	0.0368	0.0517
BA × WAI	β_{16}	-0.0209	0.0034	-0.0279	-0.0131
BA × Tmin	β_{17}	-0.0215	0.0043	-0.0287	-0.0137
BA × TA	β_{18}	0.0336	0.0034	0.0273	0.0409
BA × PA	β_{19}	-0.0130	0.0031	-0.0185	-0.0063
d _m × WAI	β_{20}	-0.0431	0.0039	-0.0506	-0.0366
d _m × Tmin	β_{21}	0.0277	0.0040	0.0195	0.0349
d _m × TA	β_{22}	-0.0107	0.0036	-0.0182	-0.0038
d _m × PA	β_{23}	-0.0031	0.0027	-0.0096	0.0021
WAI × TA	β_{24}	0.0263	0.0050	0.0143	0.0366
WAI × PA	β_{25}	0.0249	0.0040	0.0168	0.0319
Tmin × TA	β_{26}	0.0215	0.0049	0.0112	0.0309

1
2
3
4
5
6
7
8
9
10
11
12
13
14
15
16
17
18
19
20
21
22
23
24
25
26
27
28
29
30
31
32
33
34
35
36
37
38
39
40
41
42
43
44
45
46
47
48
49
50
51
52
53
54
55
56
57
58
59
60

812 **TABLES LEGENDS**

813 **Table 1.** Summary statistics of the inventory plots.

814 Mean, standard error and 95% percentiles [min., max.] of stand basal area change
815 (SBAC, m² ha⁻¹ yr⁻¹), basal area growth rate (SBA_{gain}, % yr⁻¹), basal area loss rate
816 (SBA_{loss}, % yr⁻¹), stand basal area (BA, m² ha⁻¹), mean d.b.h. (d_m, mm), water
817 availability (WAI, %), minimum temperature (Tmin, °C), temperature anomaly (TA, °C)
818 and precipitation anomaly (PA, %). Percentage of plots in boreal, temperate,
819 Mediterranean biomes is also shown.

820 **Table 2.** Alternative models of stand basal area change.

821 Comparisons of alternate models of stand basal area change (m² ha⁻¹ yr⁻¹) based on
822 Bayesian Information Criterion (BIC): (a) to test main effects including pair-wise
823 interactions between explanatory variables (Main and interaction effect models, i.e.
824 ignore the effect of each predictor variable and the interactions where the variable is
825 involved), (b) to test main effects without include pair-wise interactions between
826 explanatory variables (Main effect models, i.e. ignore the effect of each predictor
827 variable without considering any interaction), and (c) to test only the individual effect of
828 the interactions (Interactions effect models). The full models include the effects of
829 mean d.b.h., stand basal area, minimum temperature, temperature anomaly, and
830 precipitation anomaly. The best fitting model is given in ΔBIC value of zero (bold),
831 comparing the full model with models dropping the effect of the predictor variables
832 considering the main effects and/or the interactions. Thus, the alternate models ignore
833 the effects ('No') of: (a) main effects of the predictor variables and the interactions
834 where the variable is involved, (b) main effects of the predictor variables without
835 interactions or (c) interactions.

836 **Table 3.** Parameters of the final model of stand basal area change.

837 Mean estimated parameters (Parameter), standard error (SE) and lower and upper 95%
838 confidence intervals (LCI and UCI, respectively) of the final model of basal area change
839 (see Eq. (1)).

For Peer Review

1
2
3
4
5
6
7
8
9
10
11
12
13
14
15
16
17
18
19
20
21
22
23
24
25
26
27
28
29
30
31
32
33
34
35
36
37
38
39
40
41
42
43
44
45
46
47
48
49
50
51
52
53
54
55
56
57
58
59
60

Ruiz-Benito P, Madrigal-González J, Ratcliffe S, Coomes DA, Kändler G, Lehtonen A, Wirth C, Zavala MA. *Stand structure and recent climate change constrain stand basal area change in European forests: a comparison across boreal, temperate and Mediterranean biomes*

ELECTRONIC SUPPLEMENTARY MATERIAL

For Peer Review

APPENDIX 1. DESCRIPTION OF NATIONAL FOREST INVENTORIES OF SPAIN, GERMANY AND FINLAND

SPANISH NATIONAL FOREST INVENTORY

We used information from the second and third Spanish NFI (surveyed in the periods 1986-1996 and 1997-2007, respectively). The Spanish NFI plots are located on a 1 km² grid over forested regions (Villaescusa and Díaz 1998; Villanueva 2004). The time interval between surveys ranged from 6 to 13 years (mean 11.1 ± 0.9 years). Spanish NFI plots were sampled using a variable radius technique with four concentric circular subplots of radius 5, 10, 15 and 25 m. Within each subplot, trees were included in the sample according to their diameter at breast height (d.b.h.), with trees of 7.5-12.4 cm measured in the 5 m radius subplot, those of 12.5-22.4 cm in the 10 m radius subplot, those of 22.5-42.4 cm in the 15 m radius subplot, and those with d.b.h. larger or equal to 42.5 cm in the 25 m radius subplot.

GERMAN NATIONAL FOREST INVENTORY

We used information from the first and second German NFI. The German NFI uses a systematic grid of clusters, sampled in the periods 1986-1990 and 2001-2002 respectively. The size of the sample grid is 4 by 4 km, however, it is reduced in some federal states to either 2.83 by 2.83 km or 2 by 2 km. Each cluster is a quadrangle of 150 m in length with a sample plot on each corner. Trees with a d.b.h. of 10 cm or more in the first inventory and 7 cm in the second were selected by the angle-count method with a basal area factor (BAF) of 4 (m² ha⁻¹) if they are alive or recently dead.

FINNISH NATIONAL FOREST INVENTORY

We used data from the permanent sample plots of the Finnish NFI from two consecutive surveys sampled in the periods 1985-1986 and 1995 (subset NFI8). This permanent sample plot data has a systematic grid of plot clusters in forested areas (Mäkipää and Heikkinen 2003). In Southern Finland the grid is 16 by 16 square km, with four plots in each cluster at 400 m. intervals, while in Northern Finland the grid is a 24 by 32 km rectangle with three plots per cluster, at 600 m. intervals. These permanent sample plot data were sampled using a variable radius technique with two concentric circular subplots of radius 5.64 m for trees under 10.5 cm d.b.h. and 9.77 m for trees of d.b.h. 10.5 cm or higher.

REFERENCES

Mäkipää R, Heikkinen J. 2003. Large-scale changes in abundance of terricolous bryophytes and macrolichens in Finland. *Journal of Vegetation Science* 14: 497–508.

Villaescusa R, Díaz R, Ed. 1998. Segundo Inventario Forestal Nacional (1986-1996). Madrid: Ed. Ministerio de Medio Ambiente, ICONA.

Villanueva JA, Ed. 2004. Tercer Inventario Forestal Nacional (1997-2007). Comunidad de Madrid. Madrid: Ed. Ministerio de Medio Ambiente.

APPENDIX 2. FURTHER DETAILS REGARDING SELECTION OF CLIMATIC VARIABLES.

Each of the NFI plots was characterized by 22 climatic variables from WorldClim (Hijmans and others 2005) and CGIAR-CSI GeoPortal, using CGIAR-CSI Global-Aridity and Global-PET Database (Zomer and others 2007; 2008). The relationship between the initial set of highly correlated climatic variables (see Table S2) was explored using Principal Component Analysis in R (R Development Core Team, 2012). The first axis of the PCA (explaining 54% of the variance) was strongly and positively correlated with potential water availability and negatively correlated with potential evapotranspiration. The second axis (explaining 24% of the variance) was strongly correlated with mean temperature of the coldest quarter (°C) and temperature seasonality (°C). To select which indicator of climate performed better we compared single-predictor models using quadratic functional forms which individually used water availability, potential evapotranspiration, minimum temperature and temperature seasonality as predictors of stand basal area change. The best predictors of climate (according to Bayesian Information Criteria, BIC) were water availability and minimum temperatures and were retained for our modeling analysis (Table S2.1).

Table S2.1. Comparison of stand basal area change models based on BIC parameterized variables that could be used as representative of climate. Predictor variables are WAI (water availability), PET (potential evapotranspiration), Tmin (minimum temperatures) and TS (Temperature seasonality). Number of parameter (NP), Bayesian Information Criterion (BIC) and Δ BIC are also shown.

Predictor	NP	BIC	Δ BIC
WAI	3	66873	0
PET	3	67365	492
Predictor	NP	BIC	Δ BIC
Tmin	3	69166	0
TS	3	72339	3172

REFERENCES

1
2
3
4
5
6
7
8
9
10
11
12
13
14
15
16
17
18
19
20
21
22
23
24
25
26
27
28
29
30
31
32
33
34
35
36
37
38
39
40
41
42
43
44
45
46
47
48
49
50
51
52
53
54
55
56
57
58
59
60

Hijmans RJ, Cameron SE, Parra JL, Jones PG, Jarvis A. 2005. Very high resolution interpolated climate surfaces for global land areas. *International Journal of Climatology* 25: 1965-1978.

R Development Core Team. 2012. R: a language and environment for statistical computing. Vienna: R Foundation for Statistical Computing. www.r-project.org.

Zomer R, Bossio D, Trabucco A, Yuanjie L, Gupta D, Singh V. 2007. Trees and water: smallholder agroforestry on irrigated lands in Northern India. Colombo: International Water Management Institute.

Zomer RJ, Trabucco A, Bossio DA, Verchot LV. 2008. Climate change mitigation: A spatial analysis of global land suitability for clean development mechanism afforestation and reforestation. *Agriculture, Ecosystems & Environment* 126: 67-80.

For Peer Review

TABLE S1. Main characteristics of the plot and sampling design from the three National Forest Inventories used in this study (see more details in Appendix S1).

	Finland	Germany	Spain
Survey dates	1985/86 - 1995	1986/90 - 2001/02	1986/96 - 1997/2007
Sample plot design	Cluster design, number and grid size depend on location. Mostly 6 x 6 km and 7 x 7 km grid. 250 or 300 m between plots in a cluster. 10, 11 or 14 plots in a cluster	Cluster design, 4 subplots. Grid size depends on region. Standard grid size is 4 by 4 km	1 by 1 km grid of single sample plots
Sample tree survey design	Variable radius	Angle-count	Variable radius
Plot size (m ²)	100, 300	Variable, Basal Area Factor (BAF) 4 m ² ha ⁻¹	79, 315, 707, 1964
Minimum tree d.b.h. (cm)	1	10, 7	7.5
No. plots included in study (percentage)	(4.00%)	(34.48%)	(61.52%)

1
2
3
4
5
6
7
8
9
10
11
12
13
14
15
16
17
18
19
20
21
22
23
24
25
26
27
28
29
30
31
32
33
34
35
36
37
38
39
40
41
42
43
44
45
46
47

TABLE S2. List of initial set of 22 climatic predictors of stand basal area change available from WorldClim (Hijmans and others 2005) and CGIAR-CSI GeoPortal, using CGIAR-CSI Global-Aridity and Global-PET Database (Zomer and others 2007; 2008).

CODE	VARIABLE	UNITS	DEFINITION
BIO1	Annual mean temperature	°C	The mean of all the weekly mean temperatures
BIO2	Mean diurnal range	°C	The mean of all the weekly diurnal temperature ranges
BIO3	Isothermality	%	The mean diurnal range divided by the annual temperature range
BIO4	Temperature seasonality	°C	Standard deviation *100
BIO5	Max temperature of warmest month	°C	Highest temperature of any weekly maximum temperature.
BIO6	Min temperature of coldest month	°C	Lowest temperature of any weekly minimum temperature.
BIO7	Temperature annual range	°C	Difference between BIO5 and BIO6

CODE	VARIABLE	UNITS	DEFINITION
BIO8	Mean temperature of wettest quarter	°C	The wettest quarter of the year is determined (to the nearest week), and the mean temperature of this period is calculated.
BIO9	Mean temperature of driest quarter	°C	The driest quarter of the year is determined (to the nearest week), and the mean temperature of this period is calculated.
BIO10	Mean temperature of warmest quarter	°C	The warmest quarter of the year is determined (to the nearest week), and the mean temperature of this period is calculated.
BIO11	Mean temperature of coldest quarter	°C	The coldest quarter of the year is determined (to the nearest week), and the mean temperature of this period is calculated.
BIO12	Annual precipitation	mm	The sum of all the monthly precipitation estimates.
BIO13	Precipitation of wettest month	mm	The precipitation of the wettest week or month, depending on the time step.
BIO14	Precipitation of driest month	mm	The precipitation of the driest week or month, depending on the time step.
BIO15	Precipitation seasonality (coefficient of variation)	mm	The coefficient of variation is the standard deviation of the weekly precipitation estimates expressed as a percentage of the mean of those estimates (i.e. the annual mean).
BIO16	Precipitation of wettest quarter	mm	The wettest quarter of the year is determined (to the nearest week), and the total precipitation over this period is calculated.

CODE	VARIABLE	UNITS	DEFINITION
BIO17	Precipitation of driest quarter	mm	The driest quarter of the year is determined (to the nearest week), and the total precipitation over this period is calculated.
BIO18	Precipitation of warmest quarter	mm	Warmest quarter of the year is determined (to the nearest week), and the total precipitation over this period is calculated.
BIO19	Precipitation of coldest quarter	mm	The coldest quarter of the year is determined (to the nearest week), and the total precipitation over this period is calculated.
Aridity	Global potential aridity	adimensional	Quantify precipitation availability over atmospheric water demand using the ratio between mean annual precipitation and PET
WAI	Water availability index	%	Difference between precipitation and evapotranspiration relative to evapotranspiration (%)
PET	Global potential evapotranspiration	mm	$PET = 0.0023 \times RA \times (Tmean + 17.8) \times TD0.5$, where $Tmean$ is monthly temperature, RA is extra-terrestrial radiation and TD is temperature range.

TABLE S3. Mean, standard error and 95% percentiles [min., max.] for each country of the NFIs used in this study (Spain, Germany, and Finland) for: stand basal area change (SBAC, $\text{m}^2 \text{ha}^{-1} \text{yr}^{-1}$), basal area growth rate (SBA_{gain} , $\% \text{yr}^{-1}$), basal area loss rate (SBA_{loss} , $\% \text{yr}^{-1}$), stand basal area (BA, $\text{m}^2 \text{ha}^{-1}$), mean d.b.h. (d_m , mm), water availability (WAI, %), minimum temperature (Tmin, $^{\circ}\text{C}$), absolute temperature anomaly (TA, $^{\circ}\text{C}$) and relative precipitation anomaly (PA, %).

	Spain	Germany	Finland
SBAC ($\text{m}^2 \text{ha}^{-1} \text{yr}^{-1}$)	0.31 ± 0.003 [-0.29, 1.53]	0.83 ± 0.008 [-0.31, 2.57]	0.47 ± 0.009 [-0.05, 1.31]
SBA_{gain} ($\% \text{yr}^{-1}$)	3.56 ± 0.023 [0.38, 14.29]	4.64 ± 0.054 [0.86, 19.55]	4.31 ± 0.091 [0.60, 13.96]
SBA_{loss} ($\% \text{yr}^{-1}$)	0.7 ± 0.012 [0.00, 6.86]	0.35 ± 0.014 [0.00, 3.66]	0.21 ± 0.021 [0.00, 2.08]
BA ($\text{m}^2 \text{ha}^{-1}$)	10.21 ± 0.06 [0.62, 37.57]	24.57 ± 0.16 [4.00, 56.46]	10.07 ± 0.21 [0.34, 29.87]
d_m (mm)	261.84 ± 0.77 [116.00, 601.15]	296.11 ± 1.37 [111.45, 581.65]	165.31 ± 1.19 [106.98, 285.13]
WAI (%)	-30.72 ± 0.19 [-66.84, 54.56]	15.97 ± 0.3 [-18.03, 90.71]	15.69 ± 0.21 [0.55, 30.36]
Tmin ($^{\circ}\text{C}$)	5.18 ± 0.16 [-0.10, 10.50]	-0.16 ± 0.13 [-3.20, 2.00]	-9.59 ± 0.57 [-14.60, -5.40]
TA ($^{\circ}\text{C}$)	0.55 ± 0.00 [0.30, 0.90]	0.23 ± 0.00 [-0.10, 0.50]	0.1 ± 0.00 [0.00, 0.30]
PA (%)	-3.52 ± 0.02 [-9.09, 1.96]	-0.48 ± 0.03 [-6.67, 4.76]	3.73 ± 0.07 [-2.00, 8.89]

TABLE S4. BIC comparisons of stand basal area change models fitted with non-linear terms or with linear terms for each predictor variable. The full model with non-linear terms included the quadratic term of stand basal area (BA), mean d.b.h. (d_m), water availability (WAI), minimum temperature (Tmin) and precipitation anomaly (PA); and the exponential form for temperature anomaly (TA).

REML = FALSE	BIC	Δ BIC
WAI linear	57937	0
TA linear	58977	1040
Full model	58988	1051
PA linear	58981	1044
BA linear	58993	1056
Tmin linear	59259	1322
d_m linear	59591	1654

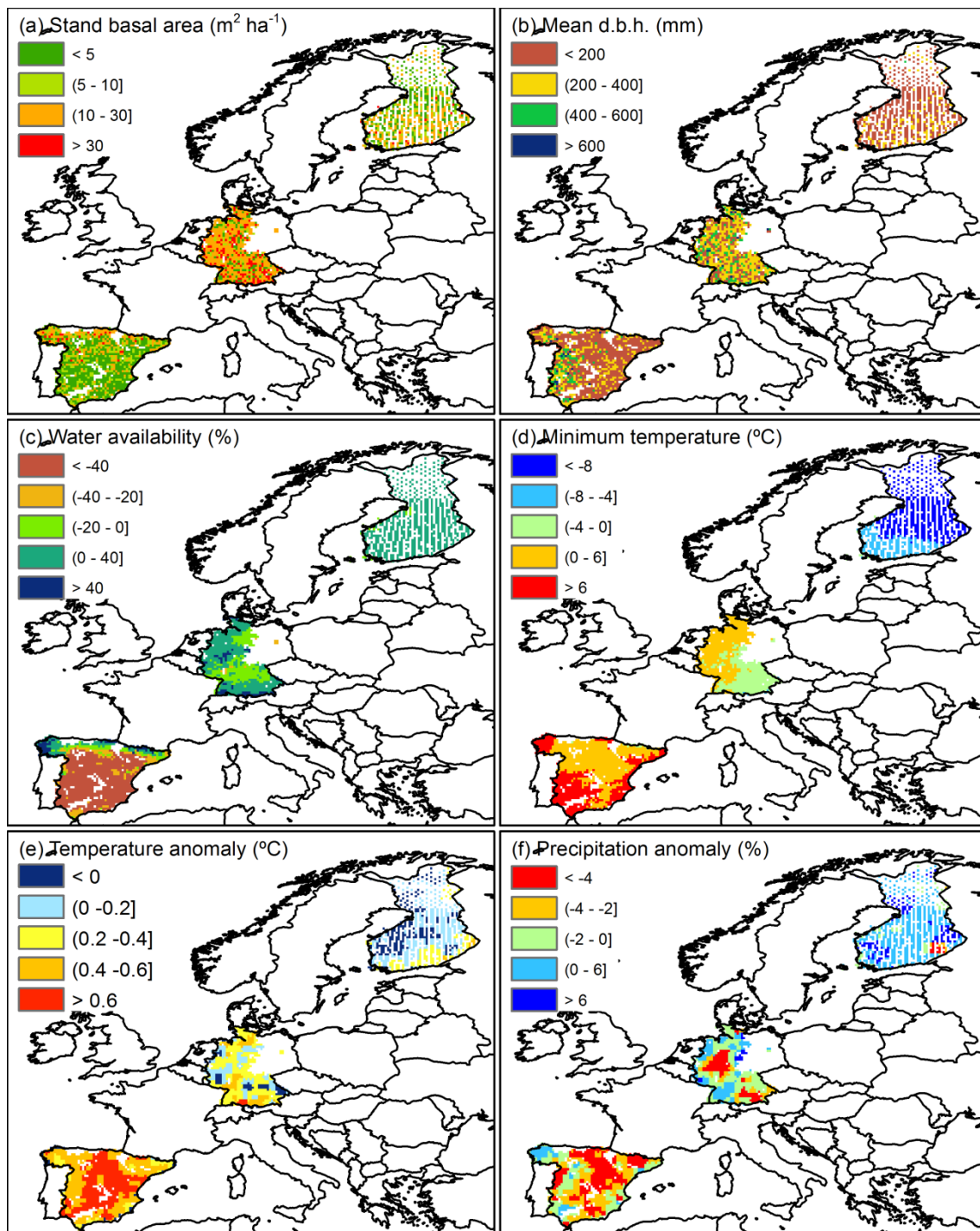


FIGURE S1. Spatial distribution of the predictor variables of stand basal area change in

the NFIs included in the study: (a) stand basal area ($\text{m}^2 \text{ha}^{-1}$), (b) mean d.b.h. (mm), (c) water availability (%), (d) minimum temperature ($^{\circ}\text{C}$), (e) absolute temperature anomaly ($^{\circ}\text{C}$), and (f) relative precipitation anomaly (%) in the Spanish, German and Finish NFIs at a spatial resolution of 0.2×0.2 degrees.

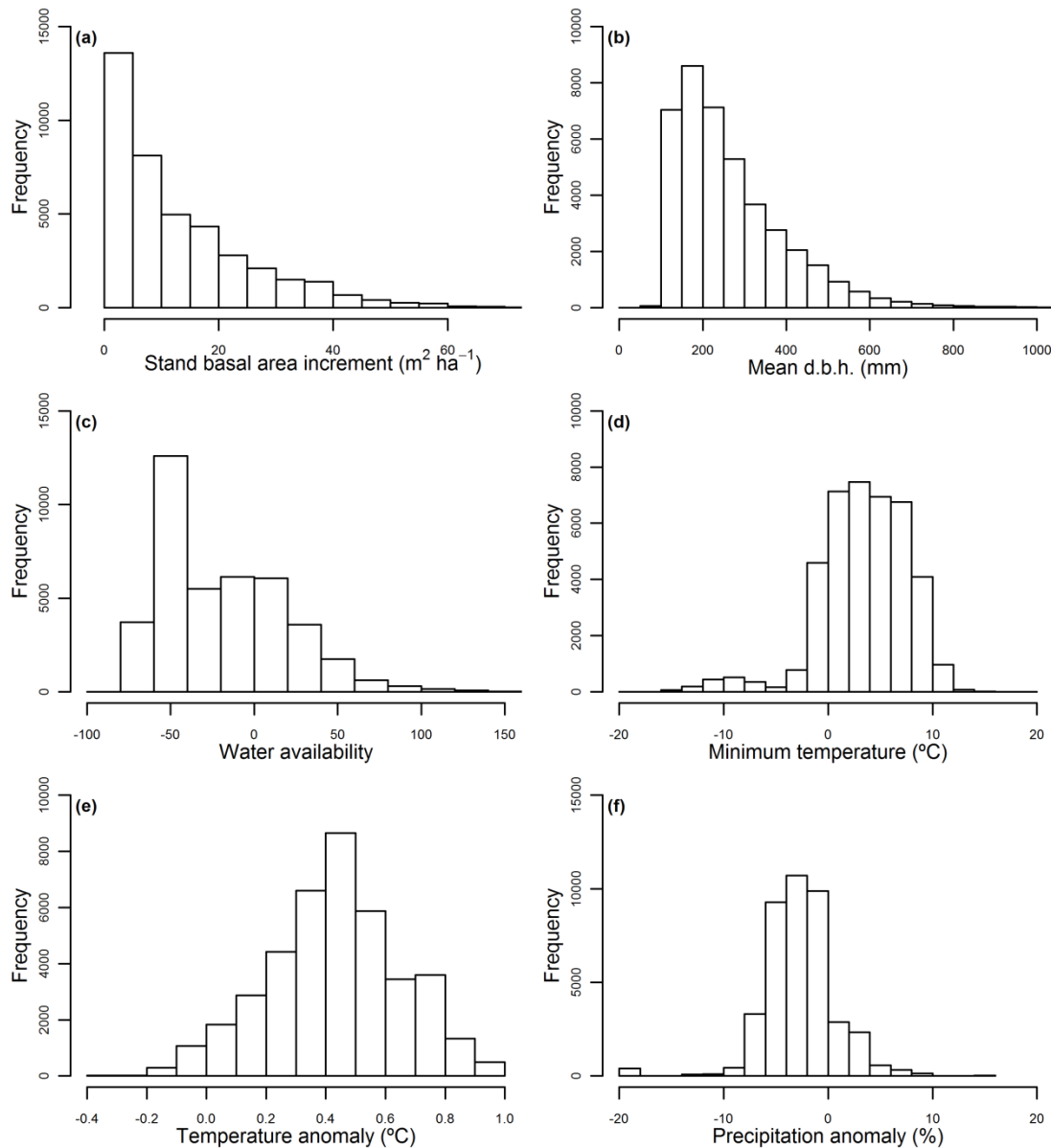


FIGURE S2. Histograms of the predictor variables of stand basal area change: (a) stand basal area ($\text{m}^2 \text{ha}^{-1}$), (b) mean d.b.h. (mm), (c) water availability (%), (d) minimum temperature ($^{\circ}\text{C}$), (e) temperature anomaly ($^{\circ}\text{C}$), and (f) precipitation anomaly (%) in the Spanish, German and Finish NFIs

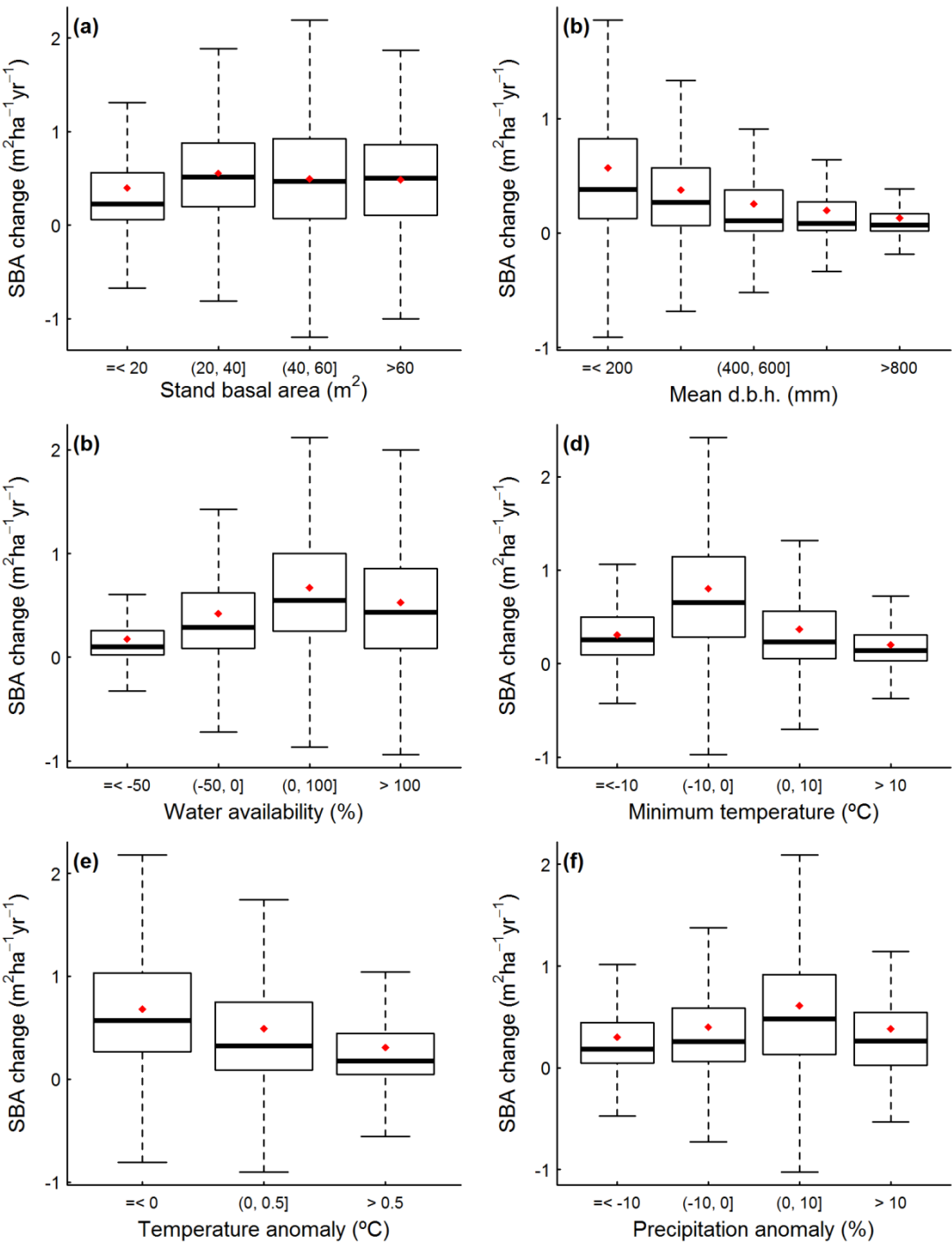


FIGURE S3. Box-whisker plots of stand basal area change ($\text{m}^2 \text{ha}^{-1} \text{yr}^{-1}$) along (a) stand basal area ($\text{m}^2 \text{ha}^{-1}$), (b) mean d.b.h. (mm), (c) water availability (%), (d) minimum temperature ($^{\circ}\text{C}$), (e) absolute temperature anomaly ($^{\circ}\text{C}$) and (f) relative precipitation anomaly (%).

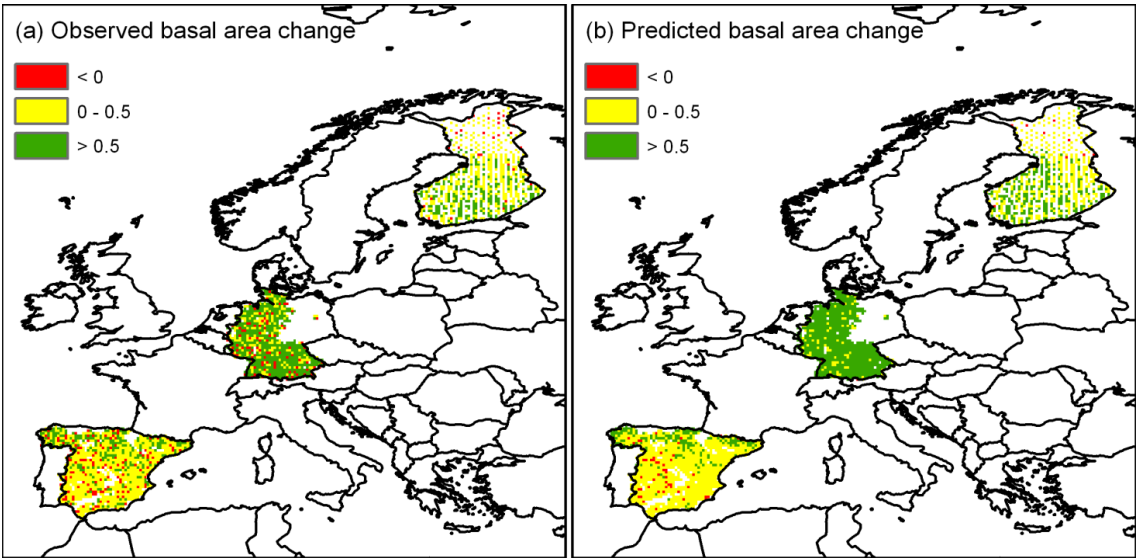


FIGURE S4. Spatial distribution of (a) observed stand basal area change ($\text{m}^2 \text{ha}^{-1} \text{yr}^{-1}$); and (b) predicted stand basal area change ($\text{m}^2 \text{ha}^{-1} \text{yr}^{-1}$) in the Spanish, German and Finnish NFIs at a spatial resolution of 0.2×0.2 degrees, showing a correlation of 0.9.

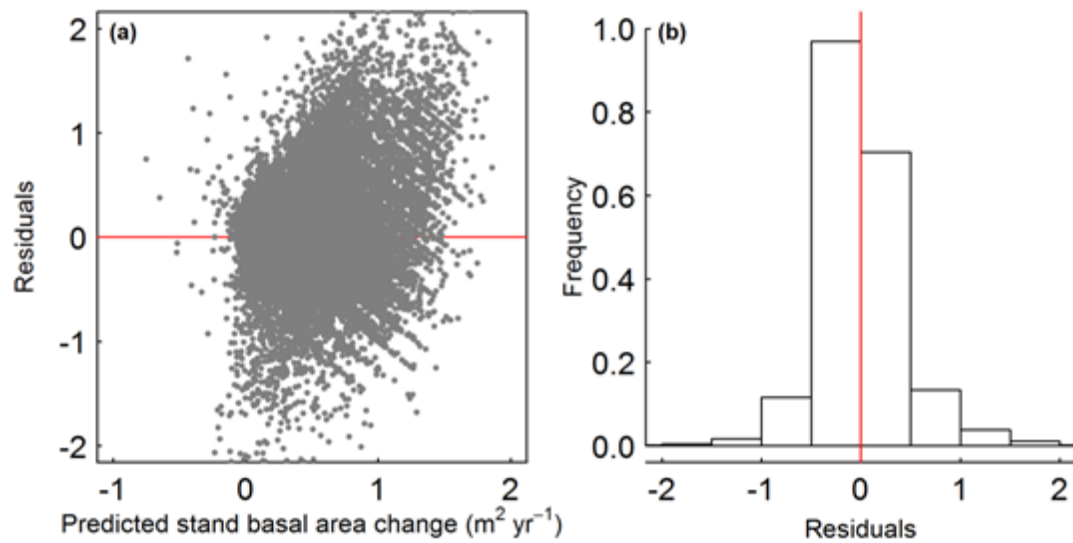


FIGURE S5. Scatterplot of residual versus predicted stand basal area change ((a), m² ha⁻¹ yr⁻¹) and histogram of the residuals (b) for the best supported model (see Eqn. 1 and parameter values in Table 3).